# Late Aptian paleoclimate reconstruction of Brazilian equatorial margin: inferences from palynology

Michelle Cardoso da Silva Giannerini[1], Marcelo de Araujo Carvalho[1], Cecília Cunha Lana[1], Gustavo Santiago[1], Natália de Paula Sá[1], Gabriel da Cunha Correia[1]

[1]Laboratorio de Paleoecologia Vegetal (LAPAV), Departamento de Geologia e Paleontologia, Museu Nacional Universidade Federal do Rio de Janeiro; 20940-040, Rio de Janeiro, Brazil.

*Corresponding author*: giannerini@gmail.com

**Abstract.**

This study conducted high-resolution paleoclimatic analyses based on the identification of palynological groups from the late Aptian age (Biozone *Sergipea veriverrucata*) in the Bragança and Codó formations within the Bragança-Viseu, São Luís, and Parnaíba basins. The analysis comprised 40 palynological samples, with 200 palynomorphs per slide counted when possible. Bioclimatic analysis was mainly supported by the identification of botanical affinities, and ecological and climatic parameters such as wet/arid trend (Fs/X), Shannon-Wiener diversity, and indicator species analysis (IndVal) were used. Statistical analyses such as principal component and cluster analyses were employed to support the paleoclimatic interpretations. The study recognized 69 genera distributed among the main groups of living plants, including bryophytes, ferns, lycophytes, gymnosperms, and angiosperms. It was possible to attribute botanical affinity in 94.2% of the taxa, and nine genera occurred in all sections studied: *Afropollis*, *Araucariacites*, *Callialasporites*, *Cicatricosisporites*, *Classopollis*, *Cyathidites*, *Deltoidospora*, *Equisetosporites*, and *Verrucosisporites*, with *Classopollis*

being the most abundant. The stratigraphic distribution of the bioclimatic groups (hydrophytes, hygrophytes, lowland tropical flora, upland flora, and xerophytes) allowed for the identification of climatic phases: pre-evaporitic, evaporites, and post-evaporites. In the pre-evaporitic phase, the most significant abundances were between the hygrophytes and upland flora, indicating a certain level of humidity. Xerophytes were the most abundant in all phases, with a conspicuous increase in the evaporitic phase, reflecting an increase in aridity. In the post-evaporitic phase, there was a significant increase in the upland flora with the return of wetter conditions. This study confirmed an increasing humidity trend in the analyzed sections, probably owing to the influence of the Intertropical Convergence Zone that already operated during the late Aptian.

## 1. Introduction

The palynoflora preserved in the upper Aptian rocks of South America and Africa is typical of hot conditions and is commonly associated with arid climates (Chumakov et al., 1995, Hay and Floegel, 2012). However, because biodiversity tends to be higher in wetter climates, the high diversity observed during the Aptian raises the possibility that this arid phase fluctuated during that age. The palynoflora related to hot and humid climates exhibits a growing trend toward these conditions, even during the Aptian. This trend may be linked to the shifting and strengthening of a humid belt associated with the Intertropical Convergence Zone (ITCZ) (Hay and Floegel, 2012; Scotese, 2016; Carvalho et al., 2022; Santos et al., 2022), as well as to the establishment of the South Atlantic, which affected the marine current system.

Palynology plays an important role in paleoclimate studies, because analyzing the assemblages of palynomorphs (e.g., spores, pollen grains), it is possible determine from the botanical affinities the types of plants that existed in the past and infer their climatic preferences. For instance, certain pollen types are indicative of wetter climates, while others are associated with drier conditions. Palynological analysis can also provide evidence of seasonal changes, temperature variations, moisture levels, and extreme climatic events. Upper Aptian rocks from Brazilian sedimentary basins, including the Bragança and Codó formations, contain a significant representation of conifers from the family Cheirolepidiaceae and their pollen grains, such as *Classopollis* (Regali et al., 1974; Carvalho et al., 2017, 2019, 2022). *Classopollis* is typically associated with arid conditions, often found in lagoons and coastal areas, and frequently associated with evaporites (Batten, 1975; Vakhrameev, 1970, 1981; Doyle et al., 1982; Hashimoto, 1995; Heimhofer et al., 2008, Carvalho et al., 2019). However, studies of the Sergipe Basin (northwestern Brazil), suggest strong fluctuations in the abundance of *Classopollis* and other xerophytic flora, with a decreasing trend toward the late Aptian accompanied by an increase in fern spores that require water for reproduction (Carvalho et al., 2017, 2019). The geographic extent of these trends remains controversial, and further investigation is required to identify possible climatic oscillations in other sedimentary basins in Brazil. Analysis of the Codó and Bragança formations, located in the Cretaceous section of the São Luís, Bragança-Viseu, and Parnaíba basins near the paleoequator, where the Intertropical Convergence Zone (ITCZ) occurs, has great potential to provide insights into this topic.

The objective of this study is to infer the paleoclimate of the late Aptian age in the Bragança-Viseu, São Luís, and Parnaíba basins, all located in equatorial areas (Fig. 1), by examining the relationships among groups of palynomorphs that are sensitive

73 climatic taxa. Furthermore, this study aimed to investigate how variations in the
74 composition of paleofloras and indicator species are linked to climatic changes such as
75 shifts in humidity and temperature, as well as other paleoenvironmental forcings.

76

77 **2. Geological settings**

78 According to Milani et al. (2007), the three sedimentary basins considered in this
79 study are grouped into large assemblies based mainly on the tectonic context in which
80 they developed: Mesozoic aborted rift basins (Bragança-Viseu and São Luís basins) and
81 Paleozoic Syneclises (Parnaíba Basin).

82 The Bragança-Viseu, São Luís, and Parnaíba basins show a similar stratigraphic
83 evolution. The Bragança-Viseu and São Luís basins are located on the equatorial margin
84 and the Parnaíba Basin in north-central Brazil (Fig. 1). The basins constitute a rift
85 system (graben and semi-graben) located between the terraines of the folding belt.
86 Together, these cover an area of approximately 645,000 $km^2$. The sedimentary
87 succession of the basins consists of Paleozoic, Mesozoic, and Cenozoic rocks. The
88 Cretaceous strata are represented by the Bragança (Bragança-Viseu and São Luís
89 basins), Grajaú, Codó, and Itapecuru Formations.

90 The Bragança Formation consists of gray medium- to coarse-grained sandstones
91 and conglomerates, with subordinate medium-grained sandstones and greenish
92 siltstones. This formation is interpreted as an alluvial fan deposit.

93 The Codó Formation is composed of dark shales, anhydrite, and calcilutites, with
94 sandstone intercalations. These deposits were assigned to a lagoonal environment.

Marine incursions are indicated by fossil contents and the occurrence of evaporitic deposits.

## 3. Late Aptian climatic evolution

The pre-evaporitic, evaporitic, and post-evaporitic phases are recognized for the late Aptian (Petri et al., 1983; Milani et al., 2007). These phases occur within the K40-K50 supersequences, and show an average maximum thickness of approximately 650 m in the studied basins. The pre-evaporitic phase is represented by carbonate and siliciclastic deposits formed in fluvial and lacustrine deltaic environments within a large proto-oceanic gulf (Petri et al., 1983; Milani et al., 2007). The peak of the evaporitic deposition is recorded in the K50 supersequence, with widespread occurrences in the Brazilian equatorial margin. The origin of these deposits is heat intensification associated with the widening of the Atlantic Ocean. These conditions caused strong evaporation, leading to a wide distribution of evaporites (mainly halite and anhydrite gypsum) in the South Atlantic basins. The post-evaporitic phase is characterized by fully marine conditions, evidenced by the rich assemblages of marine fossils. During this phase, carbonates were deposited, followed by muddy and sandy sediments, in shallow marine to slope environments (Petri et al., 1983; Milani et al., 2007).

The Bragança and Codó formations are inserted within the K40-K50 Supersequence. However, in the Bragança Formation, only the pre-evaporitic phase is recognized. On the other hand, the Codó Formation has recorded the three climatic phases (pre-evaporitic, evaporitic, and post-evaporitic) (Milani et al., 2007).

## 4. Material and methods

### 4.1. Studied sections

This study was based on core samples from three basins: Bragança-Viseu and São Luís located in the equatorial margin, and the Parnaíba Basin in north-central Brazil. All of the core samples were obtained from Petrobras (the Brazilian oil company) drilling. (Fig. 1).

The stratigraphic succession studied comprises parts of the Bragança and Codó formations. The Bragança Formation (Bragança-Viseu Basin) includes wells EGST-1 (676-1872.1 m), consisting of sandstones, siltstones, and conglomerates, and VN-1 (1287.6-1317.69 m), consisting only of sandstones (Fig. 2) (Table 1). The Codó Formation includes three section from the São Luís Basin: PR-1 (1507.6-1513.1 m), composed of sandstones and siltstones, and PE-1 (1562-1776.8 m), which has a lithology similar to that of the previous one, with the addition of calcarenites. RL-1 (1157.3-1240.3 m) is composed of sandstones, siltstones, calcarenites, and anhydrites. The fourth section, CI-1 (768-907.1 m), is from the Parnaíba Basin. CI-1 has a lithology similar to that of RL-1, but the former has a more pronounced package of anhydrites than the latter does (Fig. 2) (Table 1).

The late Aptian age of the samples is based on the *Sergipea variverrucata* Biozone recognized in two studied drill cores (PR-1 and CI-1), which is correlated with part of the upper Aptian *Globigerinelloides algerianus* Zone (Carvalho et al., 2016). In the other four sections (EGST-1, VN-1, PE-1, and RL-1), *Sergipea variverrucata* was not recognized. However, the identified floristic associations (e.g., *Afropollis jardinus*, *Araucariacites australis*, *Bennettittaepollenites regaliae*, *Equisetosporites maculosus*,

143 *Klukisporites foveolatus*, *Sergipea simplex*) are attributed to the late Aptian of Brazil
144 (Regali and Santos, 1999; Carvalho et al., 2017, 2019).
145

146 **4.2. Sample preparation**

147 The samples were prepared at the Research and Development Center of Petrobras
148 (CENPES) in Rio de Janeiro, applying the standard Petrobras method of palynological,
149 compiled by Uesugui (1979) based on Erdtman (1943, 1969) and Faegri et al. (1966).
150 Thus, in this study, most mineral constituents were dissolved by hydrochloric and
151 hydrofluoric acids before heavy-liquid separation, and the remaining organic matter was
152 sieved through a 10 µm mesh before mounting on slides. The cores are stored at
153 CENPES (Rio de Janeiro, RJ).
154

155 **4.3. Palynological analyses**

156 The samples were analyzed using a transmitted light microscope. Analysis was
157 based on the first 200 palynomorphs counted on each slide. The marine elements
158 (dinoflagellate cysts and microforaminiferal linings) were counted separately.
159 Taxonomic identification was based on the methods of Regali et al. (1974), Lima
160 (1978), Dino (1992, 1994), and Carvalho et al. (2019, 2022).
161

162 **4.4. Bioclimatic analysis**

163 Palynomorphs are useful climatic indicators (bioclimatic groups) because of their
164 botanical affinities that allow the application of the ecological preferences of taxa.
165 However, identifying the spores and pollen grains of the parent plant classified at the

family level is often challenging. This study referred to the literature (e.g., Dino, 1994; Carvalho, 2004; Souza-Lima and Silva, 2018; Jansonius et al., 1976-1996) to identify the botanical affinities of the indicator species.

On the basis of botanical affinities and inferred paleoenvironmental conditions (e.g., Dino 1992, Balme 1995; Antoniolli, 2001; Carvalho et al., 2017, Carvalho et al., 2019, Carvalho et al., 2022), this study proposes five bioclimatic groups: hydrophytes, hygrophytes, tropical lowland flora, upland flora, and xerophytes. These groups provide valuable insights into the climate and vegetation of the study area.

### 4.5. Wet-dry trend

To support the bioclimatic group distribution, we used the Fs/X (fern spores *versus* xerophytes) ratio. This ratio is based on the co-occurrence of fern spores and xerophytic palynomorphs (*Classopollis* and polyplicate gnetalean pollen); therefore, it can be used as an indicator of dry-wet trends (Carvalho et al., 2019). The ratio of fern spores to xerophytic palynomorphs (Fs/X) was calculated as Fs/X=nFs/(nFs+nX), where n is the number of specimens counted, Fs is the number of fern spores (non-reworked), and X is the number of xerophytic pollen grains. In summary, Fs/X approaching 1 implies high humidity, and that approaching -1 indicates low humidity.

### 4.6. Diversity

Shannon-Weaver diversity indices H (S) were calculated for all samples by using PAST software (Hammer et al., 2001) to provide information for interpreting

paleoclimatic trends. Diversity H(S) considers the abundance of each species and is used to characterize the diversity of the assemblages.

### 4.7. Indicator species

To characterize the climate changes during the late Aptian based on paleoflora, we employed the indicator species analysis (IndVal) method. The IndVal is a widely used measure in ecological studies to evaluate the association between a particular species and a specific habitat or environmental condition. The IndVal index quantifies the level of association between a species and a habitat by considering two components: specificity and fidelity. Specificity refers to the extent to which a species is associated with a particular habitat or condition, while fidelity represents the probability of finding a species in a habitat given its occurrence in the overall study area. The IndVal index has demonstrated successful applications in palynological studies (Caron and Jackson, 2007; Roucoux et al., 2013; Carvalho et al., 2017; Trindade and Carvalho, 2018, Leandro et al. 2020). In our study, the IndVal index was employed to assess the degree of association between taxa and specific sample groups corresponding to different paleoclimatic phases. It was calculated using the formula proposed by Dufrêne and Legendre (1997): IndValGroup k, Species j=100 × Ak,j × Bk,j, where Ak,j represents specificity, and Bk,j represents fidelity. We used PAST software (Hammer et al., 2001) to calculate these values.

To ensure that our IndVal analysis fulfilled the criteria of ordination and climate-focused approach, we grouped the samples according to three climatic phases: pre-evaporitic, evaporitic, and post-evaporitic. This allowed us to identify the specific

211 indicator species associated with each climatic phase and gain insights into the
212 vegetation that existed during the late Aptian age.

213

214 **5. Results**

215 Sixty-nine genera were identified in the 40 samples and were distributed into five
216 plant groups: bryophytes (four genera), ferns (17 genera), lycophytes (10 genera), ,
217 gymnosperms (24 genera), and angiosperms (14 genera) (Appendix 1) (Table 2).
218 Twenty indeterminate morphotypes were found in ferns and 10 in angiosperms. Of the
219 69 genera identified, nine occurred in all the wells studied: *Afropollis, Araucariacites,*
220 *Callialasporites, Cicatricosisporites, Classopollis, Cyathidites, Deltoidospora,*
221 *Equisetosporites, Verrucosisporites*. The suggested botanical affinity of the 69 genera
222 was 94.2%. The 5.8% without botanical affinity refers to the group of angiosperms.
223 All bioclimatic groups were present in the studied sections (Table 3, Appendix 2).
224 In general, the palynological assemblage is predominantly composed of the xerophytic
225 bioclimatic group, characterized by a high abundance of *Classopollis*. The average
226 abundance of xerophytes was 55.7%, ranging from 46.3% to 63.6% in the sections
227 studied (Table 4). In sequence, the upland flora had an overall average abundance of
228 18.9% (ranging from 7.8% to 26%), with *Araucariacites* being the dominant taxon. The
229 hygrophyte bioclimatic group is characterized by the presence of *Cicatricosisporites*,
230 which had an average abundance of 18.6% (ranging from 11.4% to 28.4%). By contrast,
231 the hydrophyte bioclimatic group is the least abundant, with an overall average of 0.7%,
232 and is dominated by the genus *Crybelosporites*. Regarding diversity, the Shannon-
233 Wiener indices (H') obtained for the 40 samples showed an overall average of H'= 2.0,
234 which ranged from H='1.6 in the VN-1 section to H'= 2 .2 in section PE-1 (Table 4).

The values of the wet-dry trend (Fs/X ratio) ranged from 0.19 (dry) in section CI-1 to 0.39 (wet) in EGST-1(wet) (Table 4).

### 5.1. Stratigraphic distribution of bioclimatic groups in EGST-1 well

Although xerophytes are dominant overall, EGST-1 well exhibits a higher abundance of hygrophytes (24.9%) due to moderate to high occurrences of *Cicatricosisporites*, especially at the base of the well (Fig. 3). Additionally, the abundance of hygrophytes, tropical lowland flora, and upland flora increases toward the upper sections, whereas the abundance of xerophytes decreases (Fig. 4). The Shannon-Wiener indices (H') showed an overall average of H'= 2.1, slightly above the general average (H'= 2.0). The Fs/X ratio had the highest value for all sections (0.38), above the overall average (0.28), indicating more humid conditions (Table 4).

### 5.2. Stratigraphic distribution of bioclimatic groups in VN-1 well

Similar to the EGST-1 well, the VN-1 well is composed of four samples from the Bragança Formation, in which xerophytes dominate. However, unlike the former well, hygrophytes exhibit the highest average abundance (28.4%) among all studied wells, primarily because of the abundance of trilete psilate. Despite few samples, an increasing trend of hygrophytes, tropical lowland flora, and upland flora was observed, with a significant peak in hygrophytes (Fig. 4). The average diversity of H'=1.6 is the lowest for the studied basins, below the overall average (H'= 2.0). The Fs/X ratio was 0.31, above the overall average (0.28).

### 5.3. Stratigraphic distribution of bioclimatic groups in PR-1 well

The section comprises four samples from the Codó Formation. Notably, the PR-1 well exhibits the lowest average abundance of xerophytes (46.3%) (Table 4). However, it shows the highest average abundance in the tropical lowland flora group (20.4%) of all the wells studied, driven by the presence of the genus *Afropollis*. In general, an increasing trend toward hygrophytes, upland flora, and mainly tropical lowland flora was observed (Fig. 5). The average diversity was H'= 2.1 in this well. This value is one of the highest values among all the wells studied. This high diversity is mainly attributed to the significant number of species belonging to the tropical lowland flora group. The Fs/X ratio was 0.25, slightly below the overall average (0.28) (Table 4).

### 5.4. Stratigraphic distribution of bioclimatic groups in PE-1 well

The PE-1 well shows a clear decreasing trend upward of the xerophytes, which did not exceed 20% (Fig. 6). By contrast, hygrophytes and upland flora show a conspicuous increase. Highlight for the upland flora group show an average of 26% driven by the genus *Araucariacites*. The average diversity of H'=2.2 is the highest for the basins. This average diversity is due to the many species of upland flora and hygrophytes. The Fs/X ratio was 0.28, the same as the overall average (0.28) (Table 4).

### 5.5. Stratigraphic distribution of bioclimatic groups in RL-1 well

The section consists of seven samples from the Codó Formation. The xerophytic bioclimatic group dominated the entire section, with no abrupt changes in the abundance curve observed, except at the base of the section, where the hygrophytes, tropical plain flora, and upland flora groups together reached almost 40% (Fig. 7). The

284 average diversity of H'=1.9 is the second lowest for the studied basins. The Fs/X ratio
285 was 0.24, slightly below the overall average (0.28) (Table 4).
286
287 **5.6. Stratigraphic distribution of bioclimatic groups in CI-1 well**
288 The Parnaíba Basin is represented by one well, which comprises 13 samples from
289 the Codó Formation. The palynological assemblage of this section was dominated by
290 the xerophytic bioclimatic group, with a high average of 63.6%, largely because of the
291 abundance of *Classopollis* and *Equisetosporites*. The abundance curves of bioclimatic
292 groups show that in the base occurs a balance between the xerophytes and the other
293 groups, especially the upland flora, and in the top a clear dominance of xerophyte
294 group(15.9%) (Table 4). The Fs/X ratio recorded the lowest value in all sections (0.19),
295 which was below the overall average (0.28), indicating drier conditions (Table 4).
296 However, despite this, the average diversity of H'=2.0 was one of the highest, with the
297 same value as the overall average of 2.0.
298
299 **5.7. Climatic phases**
300 All six sections were individually analyzed for palynology. However, a composite
301 section was constructed (Table 5) based on the stratigraphically evident chronological
302 distribution of the climatic phases in each studied section. The composite section of the
303 Bragança-Viseu, São Luís, and Parnaíba basins consists of 40 samples, with 24 samples
304 from the pre-evaporitic phase, eight from the evaporitic phase, and eight from the post-
305 evaporitic phase (Table 5). In general, the composite section highlights the bioclimatic
306 groups of hygrophytes (18.8%) and tropical lowland flora. The diversity and Fs/X ratio
307 curves showed strong synchrony, indicating a relation between diversity and humidity
308 (Fig. 9). No marine elements were recorded in these sections.

During the pre-evaporitic phase, there is a higher abundance of xerophytes, hygrophytes, and upland flora, but with strong oscillations observed in their respective curves. The dendrogram in Fig. 9 identifies two intervals within this phase: with significant values of xerophytes at the base but with a decreasing trend toward the top. The interval above, the xerophyte curve exhibits an upward trend. The diversity and Fs/X ratio curves show synchrony but with a decreasing trend toward the top. The indicator species (IndVal) identified for the pre-evaporitic phase, *Deltoidospora* spp. (Cyatheaceae-Dicksoniaceae) is related to the montane rainforest, suggesting more humid conditions (Table 5).

The evaporitic phase, which corresponds to the gypsum layers of the Codó Formation, is characterized by the highest average of the xerophytic bioclimatic group in the composite section (Table 5). Additionally, the average abundance of the tropical lowland flora group is also high, driven by the genus *Afropollis*. Surprisingly, the mean diversity is high during this phase, but the mean Fs/X ratio is the lowest. The high diversity in arid conditions is due to the great diversity of species in the xerophytic group, such as *Classopollis classoides*, *Equisetosporites maculosus*, and *Gnetaceaepollenites jansonius*. The IndVal for the evaporitic phase is *Afropollis* spp. related to tropical lowland flora (Table 5).

The post-evaporitic phase, which includes part of a section of the Codó Formation, is characterized by a significant decrease in the dominance of the xerophytic bioclimatic group; lower average abundance (47%) in PR-1; and the clear dominance of hygrophyte groups, including tropical lowland flora and upland flora. The dendrogram reveals a break between this phase and the evaporitic phase (Fig. 9). In general, this reflects an inversion in abundance between groups related to humidity (hygrophytes, hydrophytes, tropical flora, and upland flora) and groups related to drier conditions

(xerophytes) (Fig. 9). In this phase, the indicator species is *Deltoidospora* spp., suggesting more humid conditions for pre- and post-evaporitic phases.

## 6. Discussion

The data obtained from these sections provide clear evidence of the dominance of the xerophytic bioclimatic group during the late Aptian in Brazilian sedimentary basins. This information supports that in the literature that suggests an essentially arid climate during this age (e.g., Lima, 1983; Suguio and Barcelos, 1983; Petri, 1983; Rossetti et al., 2003; Hay and Floegel, 2012, Carvalho et al., 2017, 2019, 2022). These authors attributed this aridity to the predominance of conifers from the Cheirolepidiaceae family and their *Classopollis* pollen grains. However, climatic oscillations were identified during this age, indicated by bioclimatic groups related to the humid conditions: hydrophytes, hygrophytes, tropical lowland flora, and upland flora. A relationship between these groups has been suggested (e.g., Carvalho et al., 2017, 2019, 2022). In this study, principal component analysis (PCA) was conducted between bioclimatic groups that exhibited patterns similar to those observed in the literature (e.g., Carvalho et al., 2017, 2019, 2022). The PCA revealed a positive correlation among hygrophytes, hydrophytes, tropical lowland flora, and upland flora, whereas xerophytes show a negative relationship on the first axis (Component 1) (Fig. 10), explaining more than 70% of the variation. Component 1 characterizes the wet-dry trend.

The sections of the São Luís Basin (PE-1, RL-1, and PR-1) showed the lowest abundance of xerophytic flora, followed by the sections of the Bragança-Viseu Basin (VN-1 and EGST-1) and the CI-1 section (Parnaíba Basin) farther south (Fig. 11A). More humid conditions also were suggested by Santos et al. (2022) for the São Luís

Basin. This study utilized palynological data and PCA analysis to propose the existence of a wet phase during the late Aptian in the São Luis Basin. Through the analysis of the abundance of *Araucariacites* and fern spores, as well as the presence of the genus *Classopollis* associated with carbonate sedimentation in two semi-arid intervals, an intermediate humid interval was identified. According to Santos et al. (2022), the authors suggested that the data were sufficient to identify a pre-Albian humid belt, which challenges the view of exclusively arid Gondwana during the Aptian and supports the presence of a wet phase.

As also suggested by Carvalho et al. (2022), we compared the studied sections with sections in the Espírito Santo Basin, located much farther south (at 20°S). We found that the studied basins had a lower abundance of xerophytic flora than the Espírito Santo Basin did (Fig. 11B-C). The decreasing trend in aridity observed from the southeast (Espírito Santo Basin) to the northeast (Fig. 11B-C) coincides with the location of the hot and humid belt attributed to the ITCZ (Ohba et al., 2010, Chaboureau et al., 2012, 2014; Scotese, 2016). Notably, the approach to the ITCZ belt, where xeric restrictions are milder, reflected even in the most aridity phase, the evaporitic phase, whose indicator species was the *Afropollis* spp. of the lowland tropical flora. This indicates that the ITCZ must have had diminished aridity. The genus *Afropollis* has been associated with hot, humid climates. According to Carvalho et al. (2022), this genus exhibits the weakest negative correlation with xerophytic flora (e.g., *Classopollis*).

The ITCZ belt proposed by Scotese (2016) for the Aptian covers the entire African continental paleoequator. However, although very close, it did not reach South America (Fig. 11B). Palynological analyses conducted by Deaf et al. (2020) on the late Aptian material of the Dahab Formation (Matruh Basin, Egypt) indicated a

predominance of fern spores from the hygrophyte bioclimatic group (e.g., *Triplanosporites*, *Cicatricosisporites*) and uplands (e.g. *Deltoidospora*, *Araucariacites*), accounting for approximately 60% on average. This finding suggests that the Dahab Formation is characterized by humid conditions.

The xerophytic flora (*Classopollis* and *Equisetosporites*) in the Dahab Formation averaged approximately 25%. Considering the climatic belts proposed by Scotese (2016, 2021), this formation occurred "inside" the ITCZ, which is reflected in the prevalence of bioclimatic groups associated with more humid conditions. The abundance of xerophytic flora in the Dahab Formation was lower than that in the sections studied. This difference was particularly significant when compared with the Espírito Santo Basin, where the abundance of xerophytic flora was 87.3%, as opposed to 25% in the Dahab Formation (Fig. 11C). Notably, a significant contributor to the humidity in the Dahab Formation was likely a marine influence, which was not present in the sections studied.

## 7. Conclusion

The Aptian sections studied have well-preserved palynological diversity dominated by the genera *Classopollis* (Cheirolepidiaceae) and *Araucariacites* (Araucariaceae). Some genera of ferns are also abundant such as *Cicatricosisporites* (Anemiaceae), *Verrucosisporites* (Osmundaceae), and *Deltoidospora* (Cyatheaceae).

Five bioclimatic groups were identified and proposed for interpretation: hydrophytes, hygrophytes, tropical lowland flora, upland flora, and xerophytes. The bioclimatic groups provide evidence that the climate during the late Aptian was arid. However, when considering the distribution curves of bioclimatic groups, as well as the

indicator species (IndVal) and diversity, a clear upward trend toward increased humidity was observed.

The late Aptian age was characterized by three distinct climatic phases: pre-evaporitic, evaporitic, and post-evaporitic. During the pre-evaporitic phase, despite the dominance of xerophytic flora, there were episodes of humidity, evidenced by indicator species such as *Deltoidospora* spp. The evaporitic phase was dominated by xeric elements, although the moderate to high abundance of lowland tropical flora, confirmed by *Afropollis* spp. as an indicator species, indicated some periods of humidity. The post-evaporitic phase was marked by a lower abundance of xerophytic elements and a clear dominance of groups associated with wet conditions, mainly the upland flora, suggesting a wetter climate during this phase.

The climatic variation during the late Aptian is reflected in the palynological assemblages, with the arid phase being dominated by the genus *Classopollis* and other xerophytic bioclimatic group indicators. The wet phase is marked by a significant decrease in xerophytes and a high abundance and diversity of *Araucariacites*, fern spores, and other genera related to highland, hydrophytic, and hygrophytic bioclimatic groups. The "mirror effect" observed in the frequency curves highlights the ecological differences between the arid and humid trend groups.

According to our findings, vegetation dynamics were affected by a combination of the Intertropical Convergence Zone (ITCZ) and the opening of the South Atlantic Ocean during the late Aptian age. The influence of the ITCZ is currently stronger in the north-central region of South America. Notably, climate evolution during the late Aptian in the South Atlantic led to increased humidity, which was closely linked to plant diversity and marine influences.

## Appendices


## Acknowledgements

The research was funded by CENPES/PETROBRAS Grant No. 2017/00192-8 (to M.A.C.), registered by the National Petroleum Agency (ANP) as SAP 4600558879. We CENPES/PETROBRAS for the opportunity to study the data from wells, respectively, J.R. Maizatto (CENPES/PETROBRAS) for selecting wells and assistance with samples, and C. Medeiros and N. Reis (Geological Survey of Brazil—CPRM) for supporting us with infrastructure in accordance with the technical-scientific agreement (48035.000153/2020-38). We thank the A. Santos (iitOceaneon/UNISINOS) R.RC. Ramos (Museu Nacional/UFRJ) for their helpful comments.


## Data availability

The data and code used in this paper are deposited at CENPES, PETROBRAS, Rio de Janeiro, RJ, Brazil (wells VN-1, EGST-1, RL-1, PE-1, CI-1, and PR-1). Additional information on samples (wells VN-1, EGST-1, RL-1, PE-1, CI-1 and PR-1) can be accessed in www.anp.gov.br.

## Author contributions

M.C.S.G and M.A.C. led the writing with contributions of all coauthors; M.C.S.G., C.C.L, G.S., N.P.S. and G.C.C. collected the palynological data and M.C.S.G. and M.A.C. carried out the pollen data analysis.

## Competing interests

The authors declare no competing interests.

## References


Antonioli L.: Estudo palinocronoestratigráfico da Formação Codó – Cretáceo Inferior do Nordeste brasileiro, PhD thesis. Universidade Federal do Rio de Janeiro, Rio deJaneiro, Brazil, 265 pp., 2001.

Balme B.E.: Spores and pollen grains from the Mesozoic of Western Australia. C.S.I.R.O, Australia, Commonwealth Scientific and Industrial Research Organization. Coal Research Section. Reference, Melbourne, T.C., 25, 1-48, 1957.

Balme B.E.: Fossil in situ spores and pollen grains: an annotated catalogue. Rev. Palaeobot. Palynol., 87, 81-323, 1995.

Batten D.J.: Wealden palaeocology from the distribution of plant fossils. Proc. Geol. Ass., 85, 433-458, 1975.

Caron, J.-B., Jackson, D.A.: Paleoecology of the Greater Phyllopod Bed community, Burgess Shale. Palaeogeogr. Palaeoclimatol. Palaeoecol. 258, 222–256, 2007.

Carvalho M. C., Lana C. C., Bengtson P., Sá, N. P.: Late Aptian (Cretaceous) climate changes in northeastern Brazil: A reconstruction based on indicator species analysis (IndVal). Palaeogeogr. Palaeoclimatol. Palaeoecol.485, 553-560, 2017.

Carvalho M.A.: Palynological assemblage from Aptian/Albian of the Sergipe Basin: paleoenvironmental reconstruction. Rev. Bras. Paleontol., 7, 159-168, 2004.

Carvalho M.A., Bengtson P., Lana C.C., Sá, N.P., Santiago G., Giannerini M.C.S.: Late Aptian (Early Cretaceous) dry-wet cycles and their effects on vegetation in the South Atlantic: Palynological evidence. Cretaceous Res., 100, 172-183, 2019.

Carvalho, M.A., Bengtson, P., Lana, C.C.: Late Aptian (Cretaceous) paleoceanography of the South Atlantic Ocean inferred from dinocyst communities of the Sergipe Basin, Brazil. Paleoceanography, 31, 2–26, 2016

Carvalho, M.A., Lana, C.C., Sá, N.P, Santiago, G., Giannerini, M.C.S, Bengtson P.: Influence of the intertropical convergence zone on early Cretaceous plant distribution in the South Atlantic. Sci. Rep. 12, 12600, 2022.

Chaboureau, A.-C., Donnadieu, Y., Sepulchre, P., Robin, C., Guillocheau, F., Rohais, S.: The Aptian evaporites of the South Atlantic: A climatic paradox?. Clim. Past, 8, 1047–1058, 2012.

Chaboureau, A.-C., Sepulchre, P., Donnadieu, Y., Franc, A.: Tectonic-driven climate change and the diversification of angiosperms. PNAS 111, 14066–14070, 2014.

Chumakov, N.M., Zharkov, M.A., Herman, A.B., Doludenko, M.P., Kalandadze, N.N., Lebedev, E.A., Ponomarenko, A.G., Rautian, A.S.: Climate belts of themid-Cretaceous time. Stratigr. Geol. Correl., 3, 241–260, 1995.

Dino R.: Palinologia, bioestratigrafia e paleoecologia da Formação Alagamar- Cretáceo da Bacia Potiguar, Nordeste do Brasil, PhD. thesis, Universidade de São Paulo, Brazil, 299 pp., 1992.

Dino R.: Algumas espécies novas de grãos de pólen do Cretáceo Inferior do nordeste do Brasil. Bol. Geociênc. Petrobras, 8, 257-273, 1994.

Doyle J.A., Jardiné S., Dorenkamp A.: *Afropollis*, a new genus of early angiosperm pollen, with notes on the Cretaceous palynostratigraphy and paleoenvironments of

northern Gondwana. Bull. Centres Rech. Explor. Prod. Elf-Aquitaine, 6, 39–117, 1982.

Dufrêne M., Legendre, P.: Species assemblages and indicator species: the need for a flexible asymmetrical approach. Ecol. Monogr. 67, 345–366, 1997.

Erdtman G.: An introduction to pollen analysis. Waltham, Chronica Botanica Company, v. XII, 239 p. 1943

Erdtman G.: Handbook of Palynology: An Introduction to the Study of Pollen Grains and Spores. Copenhagen, Ejnar Munksgaard, 486 pp., 1969.

Faegri K., Iversen, J.: Textbook of Pollen Analysis. Munksgaard (Scandinavian University Books), Copenhagen, 236 Pp. 1966.

Fossilworks. http://fossilworks.org, last access: 27 August 2022.

Hammer O., Harper D.A.T., Ryan P.D.: PAST: paleontological statistics software package for education and data analysis. Palaeontol. Electron., 4: 1-9, 2001.

Hashimoto A.T.: Contribuição ao estudo do relacionamento da palinologia e a estratigrafia de sequências. Análise da seção do Cretáceo Médio/Superior da Bacia de Santos. MSc. thesis, Universidade Federal do Rio Grande do Sul, Rio Grande do Sul, Brazil, 130 pp., 1995.

Hay W.W. and Floegel S.: New thoughts about the Cretaceous climate and oceans. Earth-Sci. Rev., 115, 262-272, 2012.

Heimhofer U., Adatte T., Hochuli P.A., Burla S., Weissert H.: Coastal sediments from the Algarve: low-latitude climate archive for the Aptian—Albian. Int. J. Earth Sci., 97, 785–797, 2008.

Jansonius, J., Hills, L. V. & Hartkopf-Fröder, C.: Genera File of Fossil Spores and Pollen, Spec. Pub., Department of Geology, University of Calgary, Alberta, 1976–1996.

525 Leandro, L.M, Santos, A., Carvalho, M.A., Fauth, G.: Middle to late Miocene
526 Caribbean dinoflagellate assemblages and palynofacies (DSDP Leg 15 Site 153)
527 Mar. Micropaleontol. 160, 101898, 2020.
528 Lima M. R.: Palinologia da Formação Santana (Cretáceo do nordeste do Brasil). II.
529 Descrição sistemática dos esporos da Subturma Azonotriletes. Ameghiniana, XV,
530 333-365, 1978.
531 Lima M.R.: Paleoclimatic reconstrution the Brazilian Cretaceous based on
532 palynological date. Rev. Bras. Geoc., 4, 223-228, 1983.
533 Lima, M. R.: Palinologia da Formação Santana (Cretáceo do nordeste do Brasil). II.
534 Descrição sistemática dos esporos da Subturma Zonotriletes e Turma Monoletes,
535 e dos polens das turmas Saccites e Aletes. Ameghiniana, XVI, 27-63, 1979.
536 Milani, E. J., Rangel, H. D., Bueno, G. V., Stica, J. M., Winter, W. R., Caixeta, J. M.,
537 Neto, O. P.: Bacias sedimentares brasileiras: cartas estratigráficas. Bol. Geoc.
538 PETROBRAS, 15, 183-205, 2007.
539 Ohba, M. and Ueda, H.: AGCM study on effects of continental drift on tropical climate
540 at the early and late Cretaceous. J. Meteorol. Soc. Jpn. 88, 869–881, 2010.
541 Petri S.: Brazilian Cretaceous paleoclimates: evidence from clay-minerals, sedimentar
542 structures and palynomorphs. Rev. Bras. Geoc., 13, 215-222, 1983.
543 Regali M.S.P., Uesugui N., Santos A.S.: Palinologia dos sedimentos Meso-cenozoicos
544 do Brasil (I). Bol. Téc. Petrobras, 17, 177-191, 1974.
545 Regali, M.S.P., and Santos, P.R.S.: Palinoestratigrafia e geocronologia dos sedimentos
546 albo-aptianos das bacias de Sergipe e Alagoas – Brasil. in: Simpósio sobre o
547 Cretáceo do Brasil, 5, Rio Claro, 1999, Rio Claro, Brazil, 411-419, 1999.

548 Roucoux, K.H., Lawson, I.T., Jones, T.D., Baker, T.R., Honorio Coronado, E.N.,
549 Gosling, W.D.: Vegetation development in an Amazonian peatland. Palaeogeogr.,
550 Palaeoclimatol., Palaeoecol. 374, 242–255, 2013.
551 Rossetti D.F., and Góes A. M.: Caracterização paleoambiental de depósitos albianos na
552 borda Sul da Bacia de São Luís-Grajaú: modelo de delta fluvial influenciado por
553 tempestade. Braz. J. Geol., 33, 299-312, 2003.

554 Santos, A., De Lira Mota, M., Kern, H.P., Fauth, G., Paim, P.S.G., Netto, R.G.,
555 Sedorko, D., Lavina, E.L.C., Krahl, G., Fallgatter, C., Silveira, D.M., Aquino,
556 C.D., Santos, M.O., Baecker-Fauth, S., Vieira, C.E.L.: Earlier onset of the early
557 Cretaceous equatorial humidity belt. Glob. Planet. Change, 260, 103724, 2022.

558 Scotese, C.: A new global temperature curve for the Phanerozoic. Paper Presented at the
559 Geological Society of America, Annual Meeting in Denver, Colorado – 287167,
560 2016.

561 Scotese, C. R., Song, H., Mills, J. W. & van der Meer, D. G.: Phanerozoic
562 paleotemperatures: The earth's changing climate during the last 540 million years.
563 Earth Sci. Rev. 215, 10350otese, 2021

564 Souza-Lima, W., and Silva, R. O.: Aptian-Albian paleophytogeography and
565 paleoclimatology from Northeastern Brazil sedimentary basins. Rev. Palaeobot.
566 Palyno. 258, 163–189, 2018.
567 Suguio K., and Barcelos J. H.: Paleoclimatic evidence from the Bauru Group,
568 Cretaceous of the Paraná Basin, Brazil. Rev. Bras. Geoc., 13, 232-236, 1983.

569 Trindade, V.S.F., Carvalho, M.A.: Paleoenvironment reconstruction of Parnaíba Basin
570 (north, Brazil) using indicator species analysis (IndVal) of Devonian
571 microphytoplankton. Mar. Micropaleontol. 140, 69–80, 2018.
572 Uesugui N.: Palinologia: técnica de tratamento de amostras. Bol. Téc. Petrobras, 22:
573 229-240, 1979.
574 Vakhrameev V.A.: Range and paleoecology of Mesozoic conifers. The
575 Cheirolepidiaceae. Paleontol. J. 41, 11–25, 1970.
576 Vakhrameev V.A.: Pollen *Classopollis*: indicator of Jurassic and Cretaceous climates.
577 Paleobotanist, 28, 301–307, 1981.
578
579

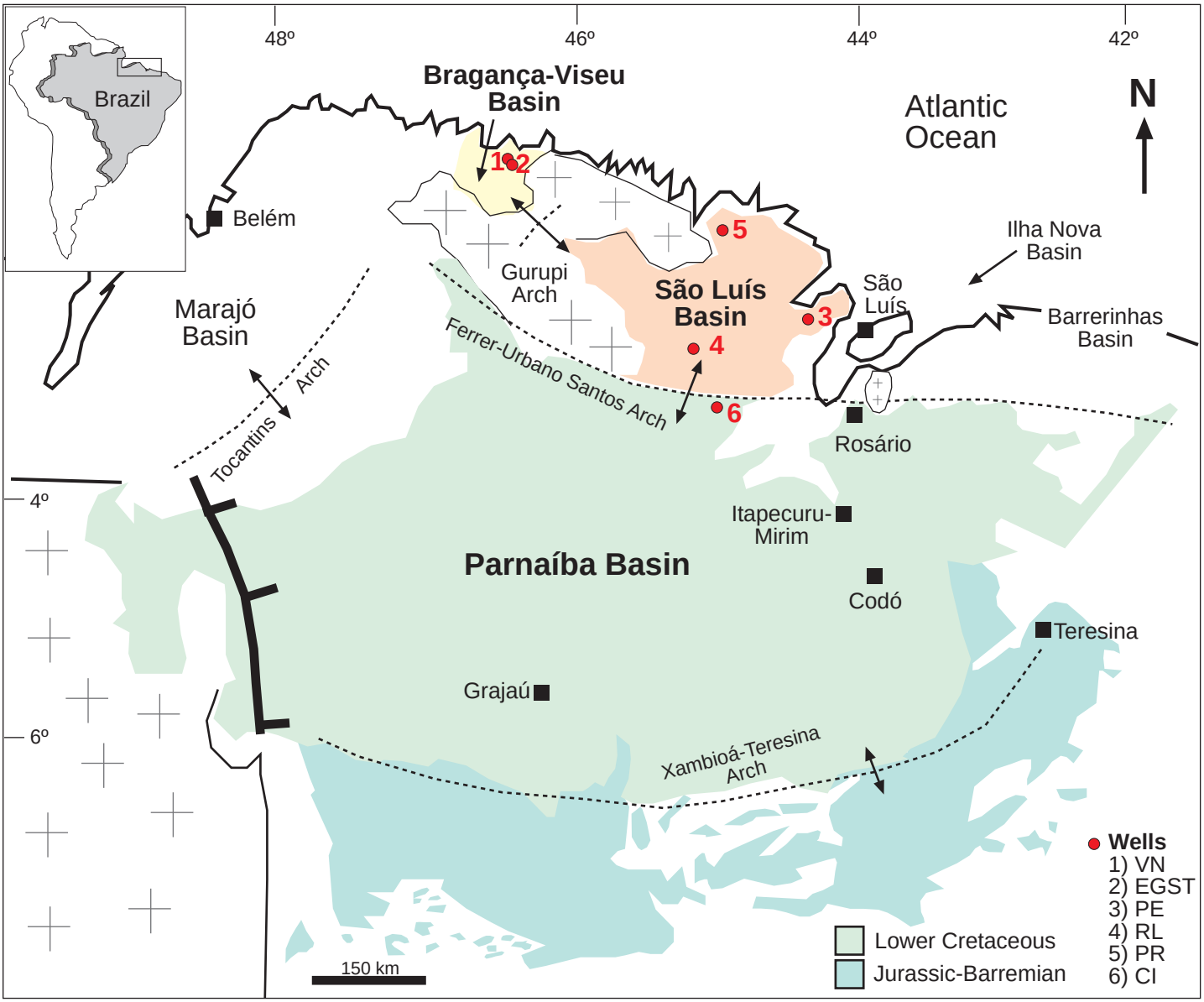
Brazil
48º
46º
44º
42º
Bragança-Viseu Basin
Atlantic Ocean
N
1
2
Belém
5
Ilha Nova Basin
Gurupi Arch
São Luís Basin
São Luís
3
Barrerinhas Basin
Marajó Basin
4
Ferrer-Urbano Santos Arch
Tocantins Arch
6
Rosário
4º
Itapecuru-Mirim
Parnaíba Basin
Codó
Teresina
Grajaú
6º
Xambioá-Teresina Arch
150 km
Wells
1) VN
2) EGST
3) PE
4) RL
5) PR
6) CI
Lower Cretaceous
Jurassic-Barremian

**A**

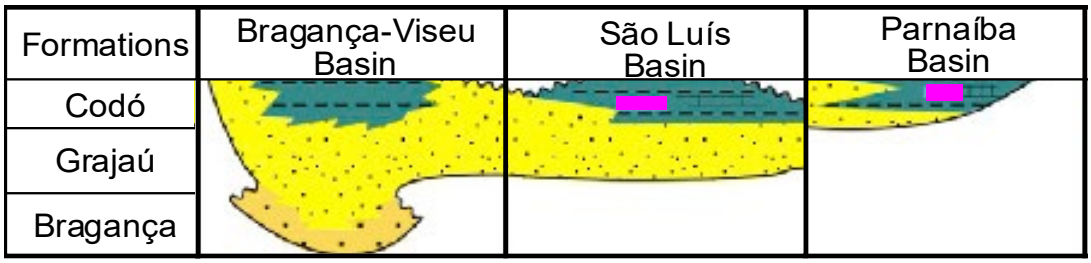


**B**

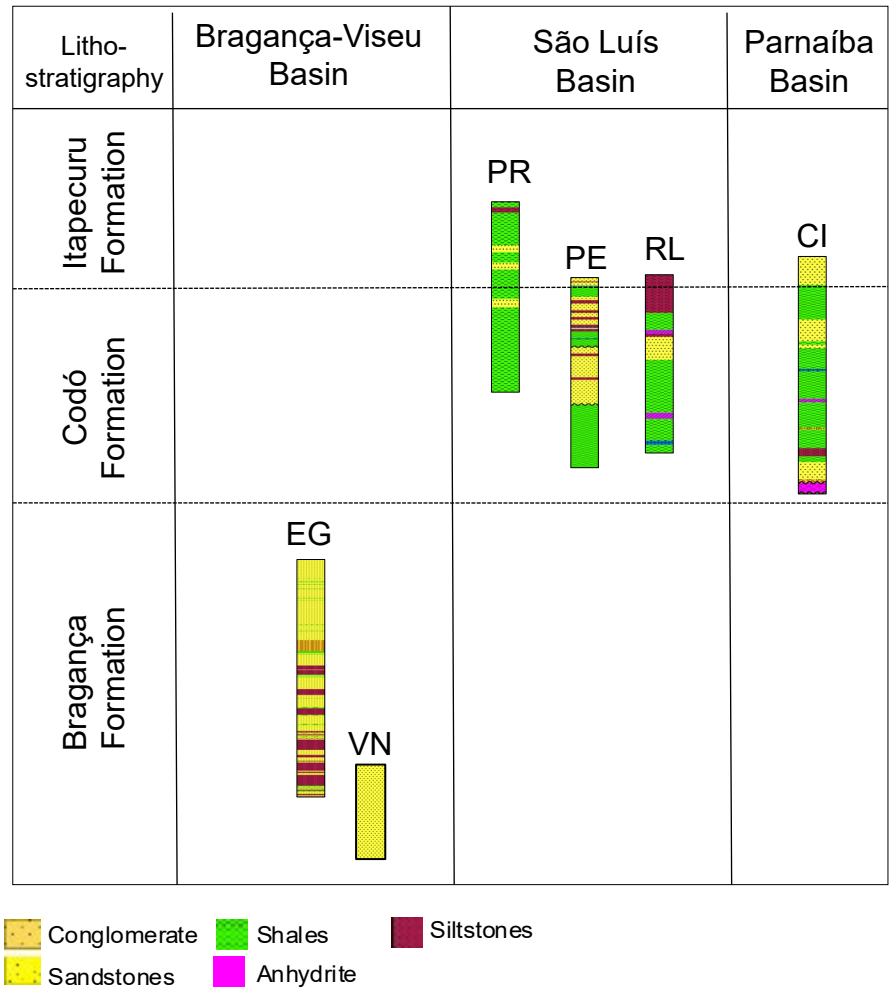


Figure 2. A) Correlation of lithostratigraphic data of the studied basins and; B) the studied wells.

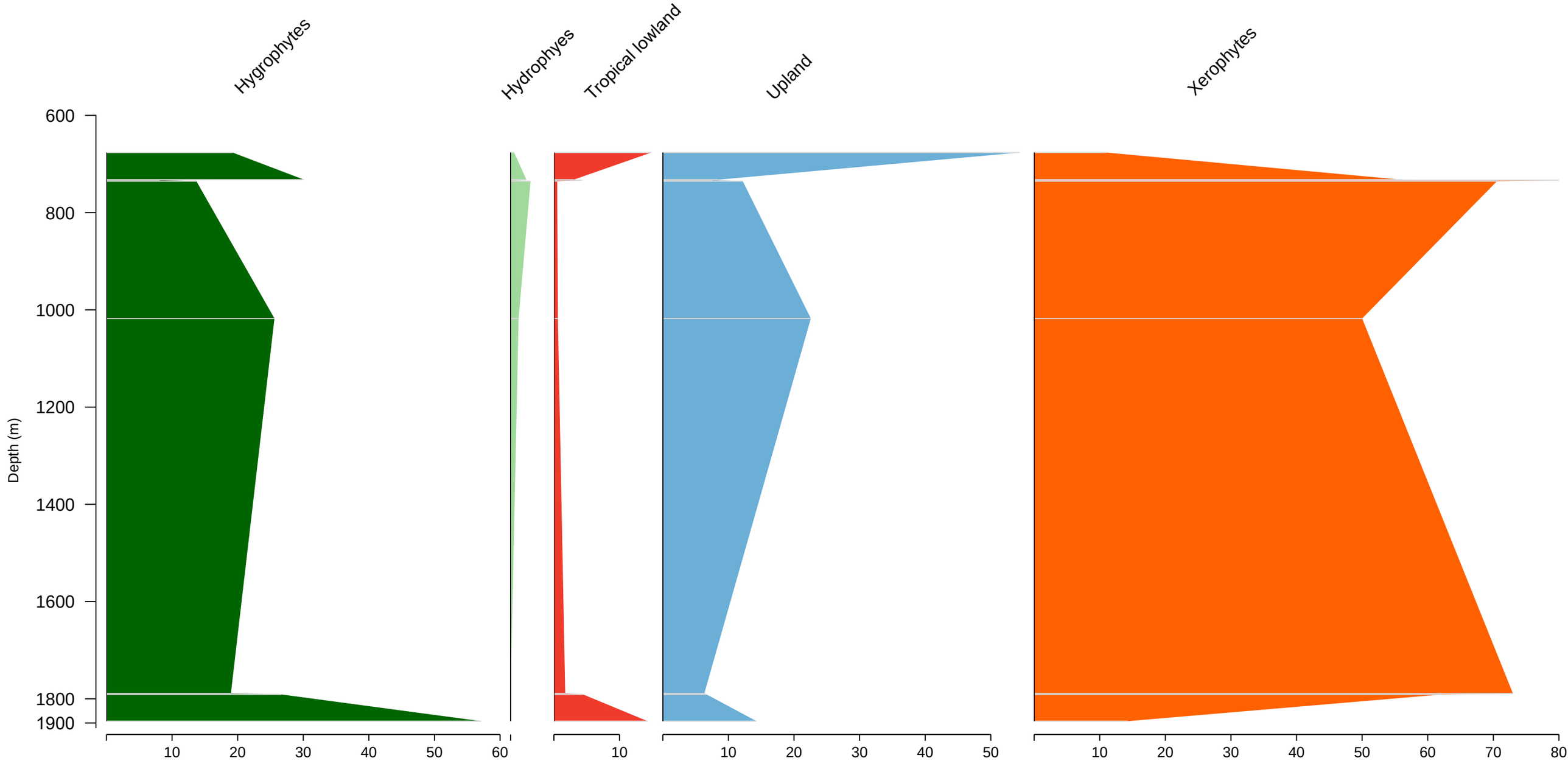


Figure 3. Stratigraphic distribution of bioclimatic groups of well EGST-1 (Bragança-Viseu Basin).

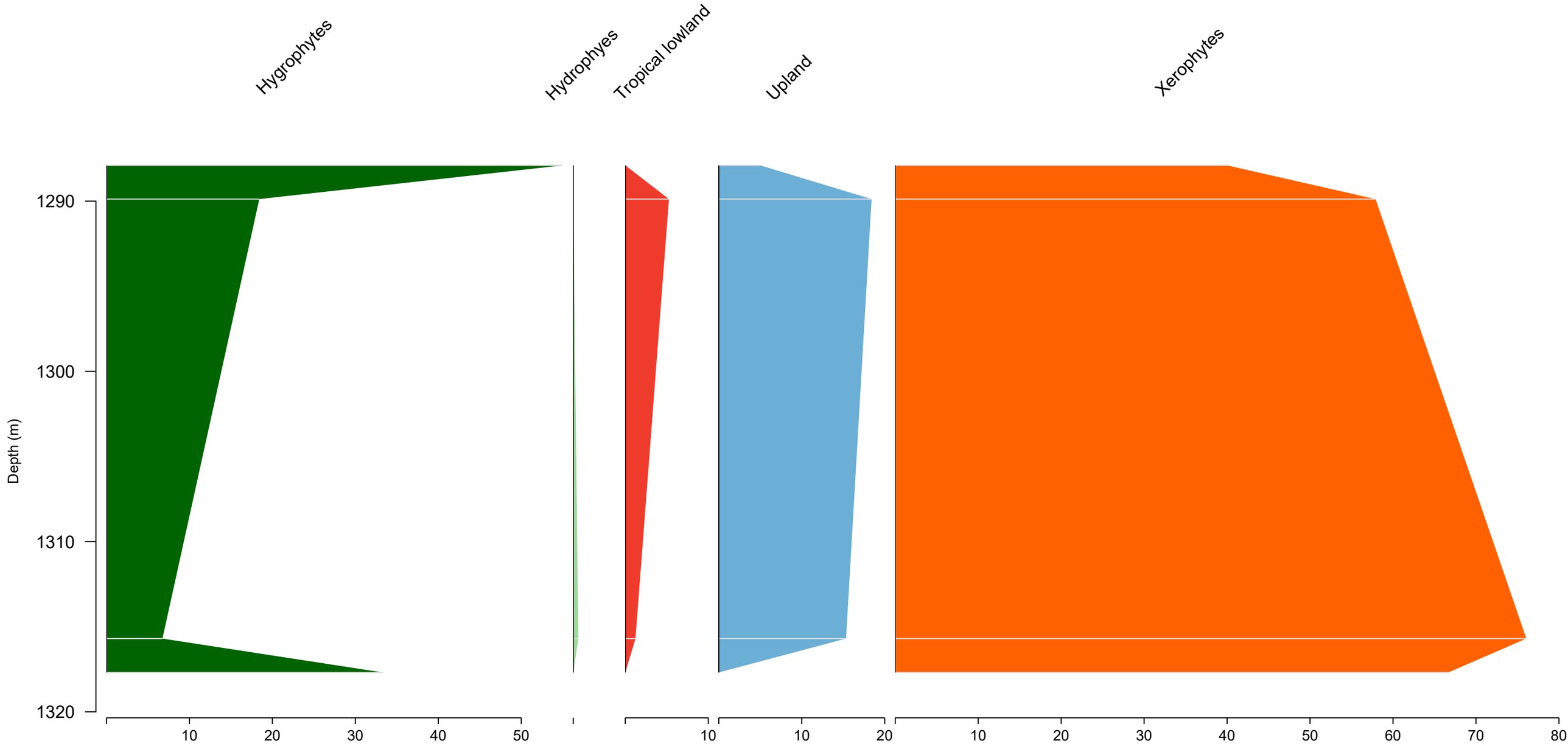


Figure 4. Stratigraphic distribution of bioclimatic groups of well VN-1 (Bragança-Viseu Basin).

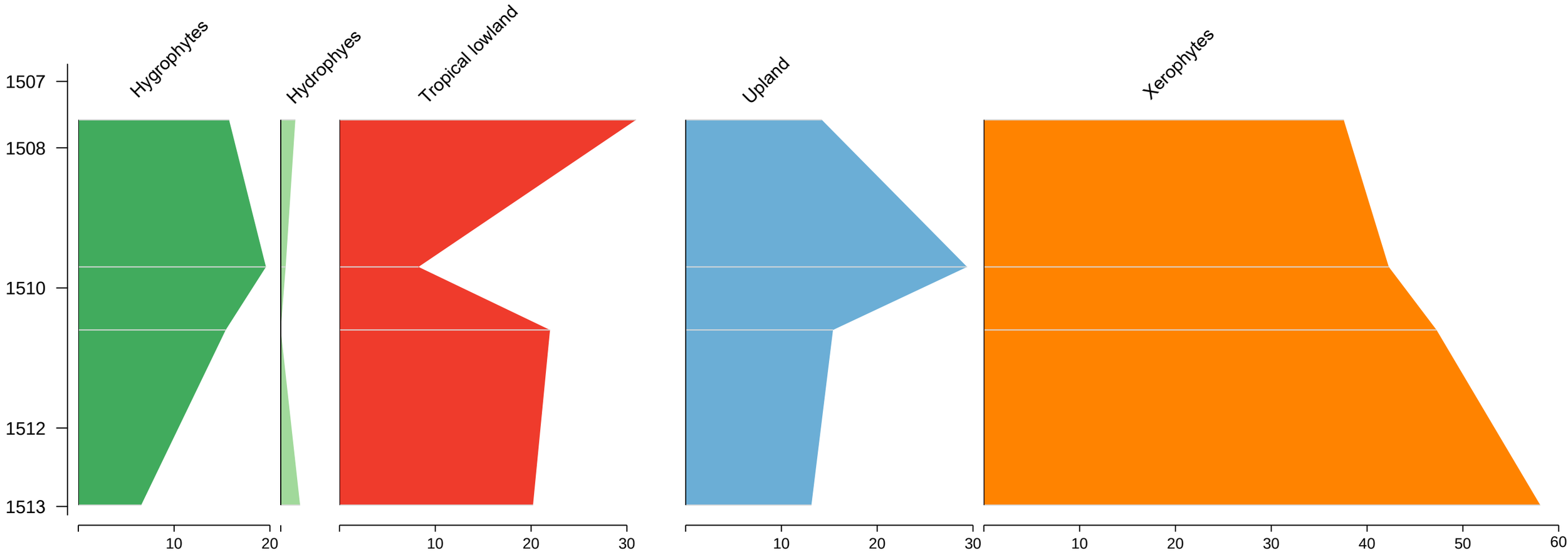


Figure 5. Stratigraphic distribution of bioclimatic groups of well PR-1 (São Luís Basin).

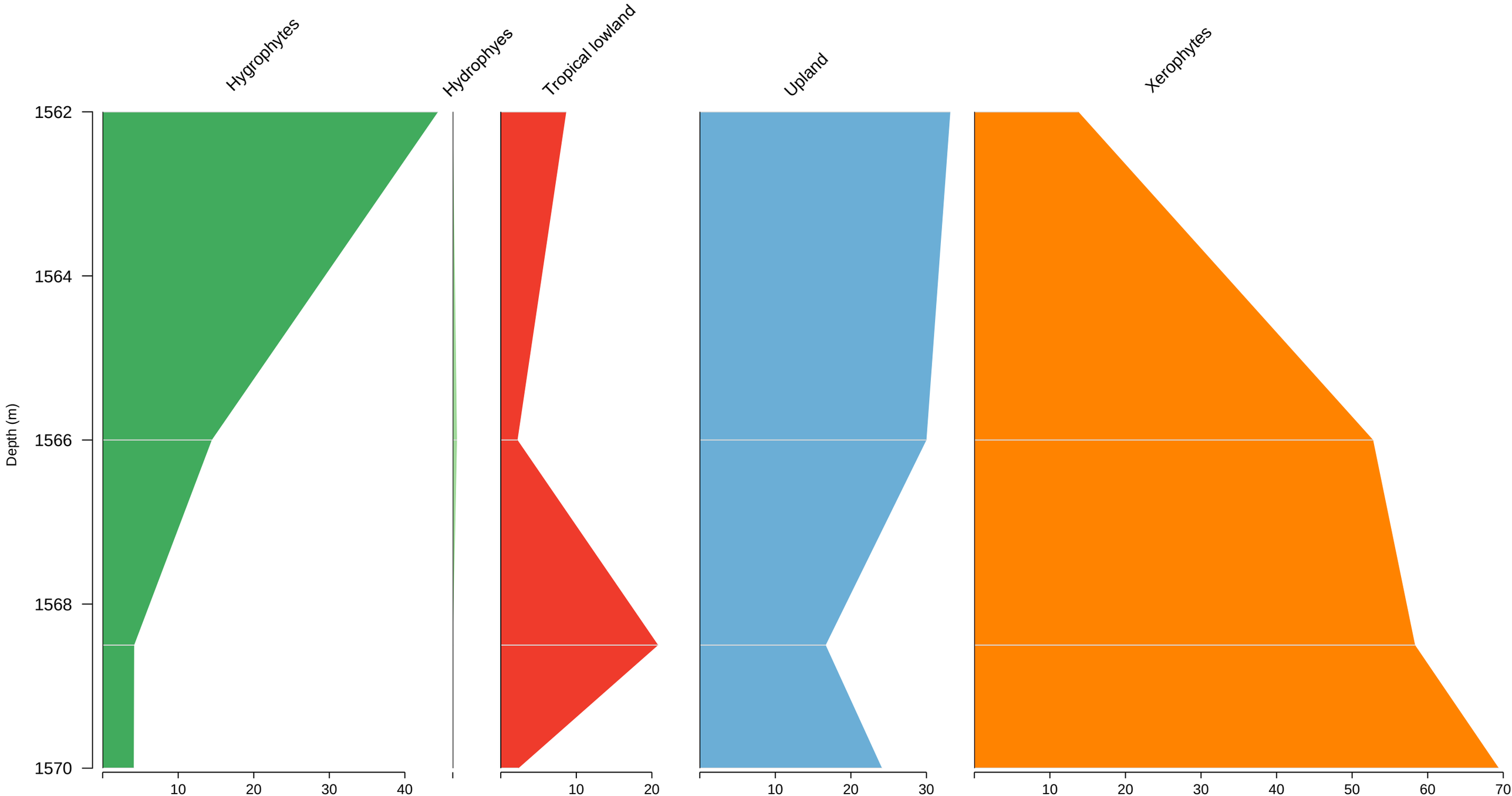


Figure 6. Stratigraphic distribution of bioclimatic groups of well PE-1 (São Luís Basin).

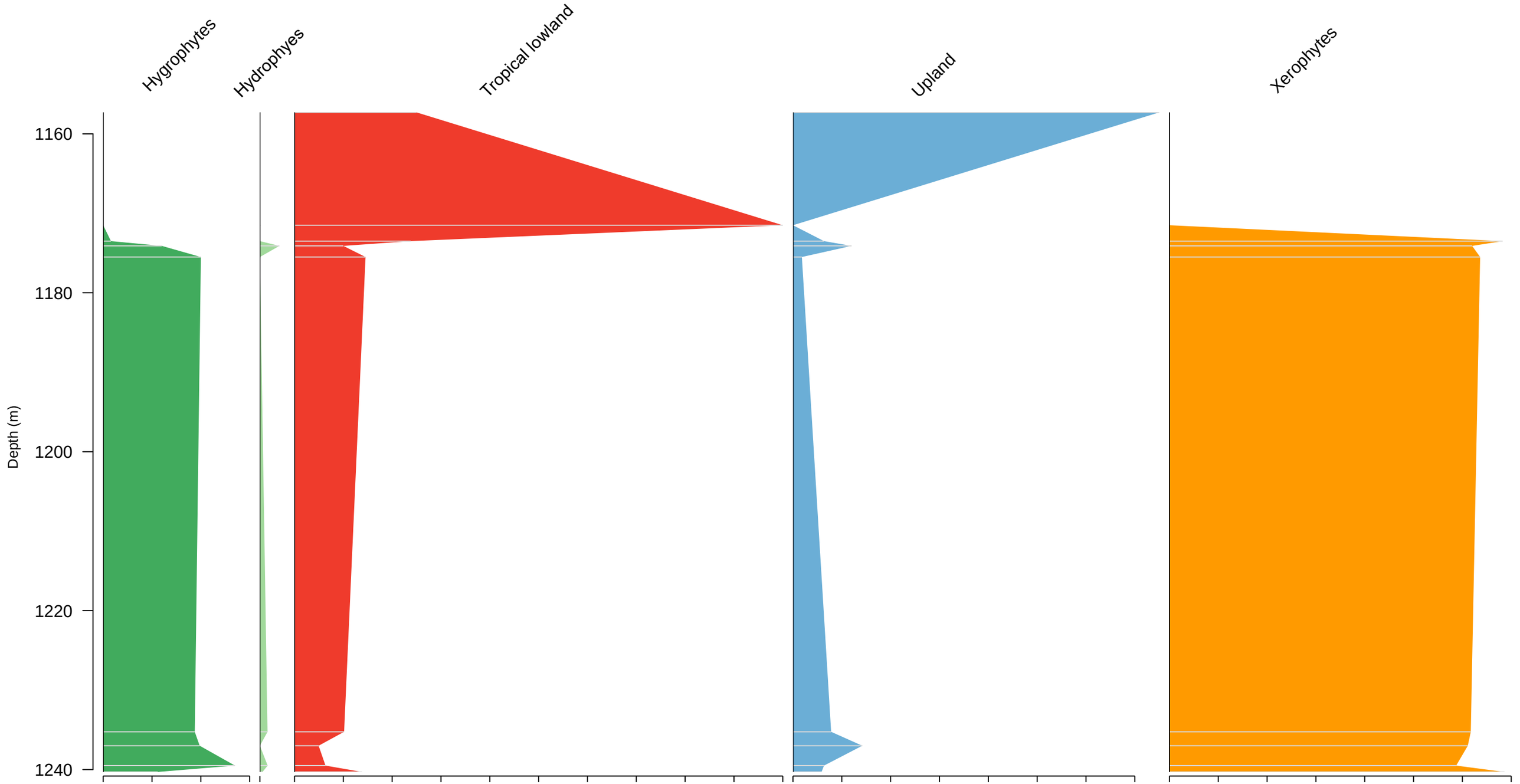


Figure 7. Stratigraphic distribution of bioclimatic groups of well RL-1 (São Luís Basin).

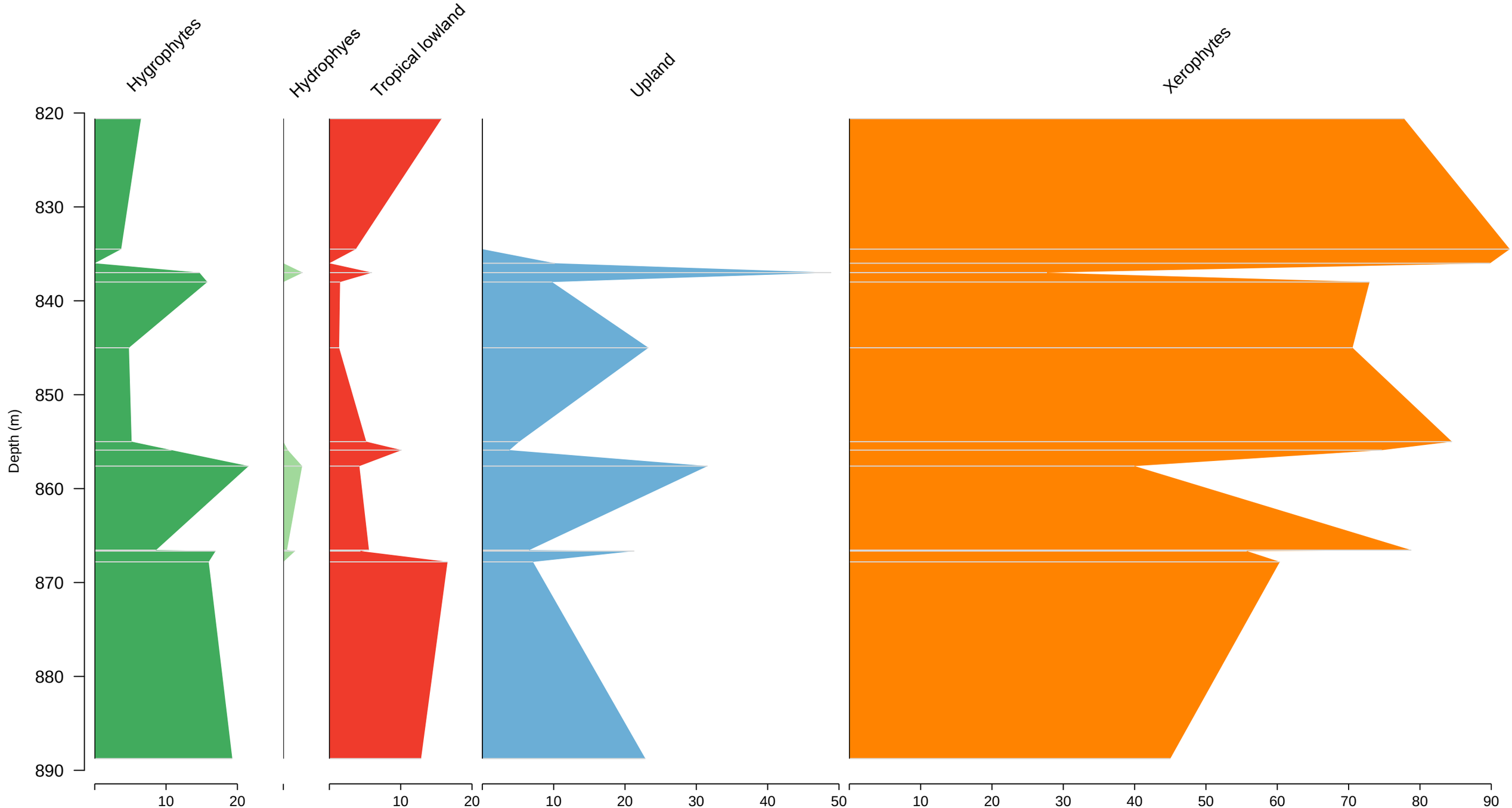


Figure 8. Stratigraphic distribution of bioclimatic groups of well CI-1 (Parnaíba Basin).

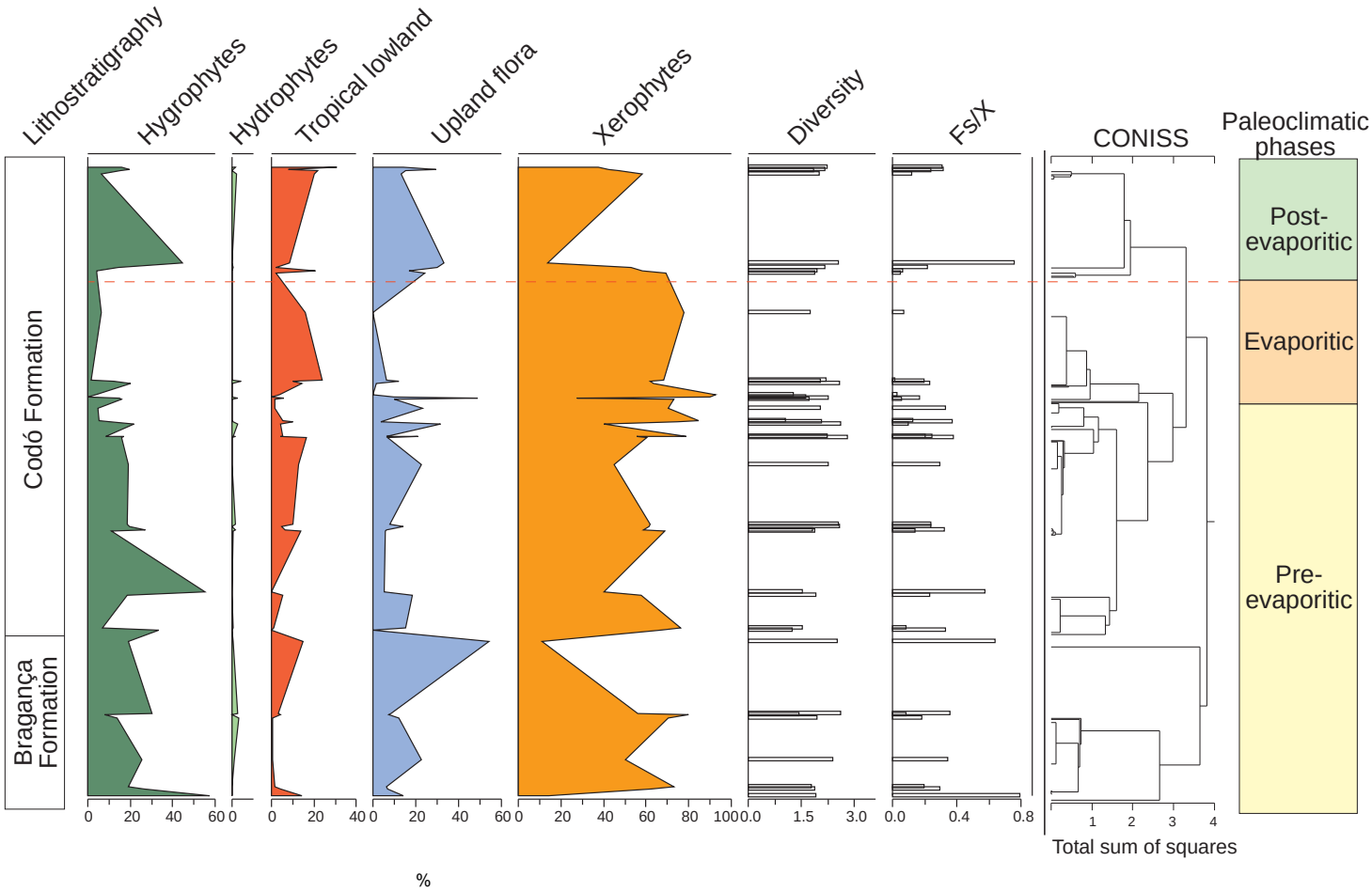


Figure 9. Composite profile showing the stratigraphic distribution of bioclimatic groups, diversity, Fs/X against the paleoclimatic phases. Agglomerative, hierarchical clustering and stratigraphically constrained dendrogram (CONISS) showing the main break (dashed red line).

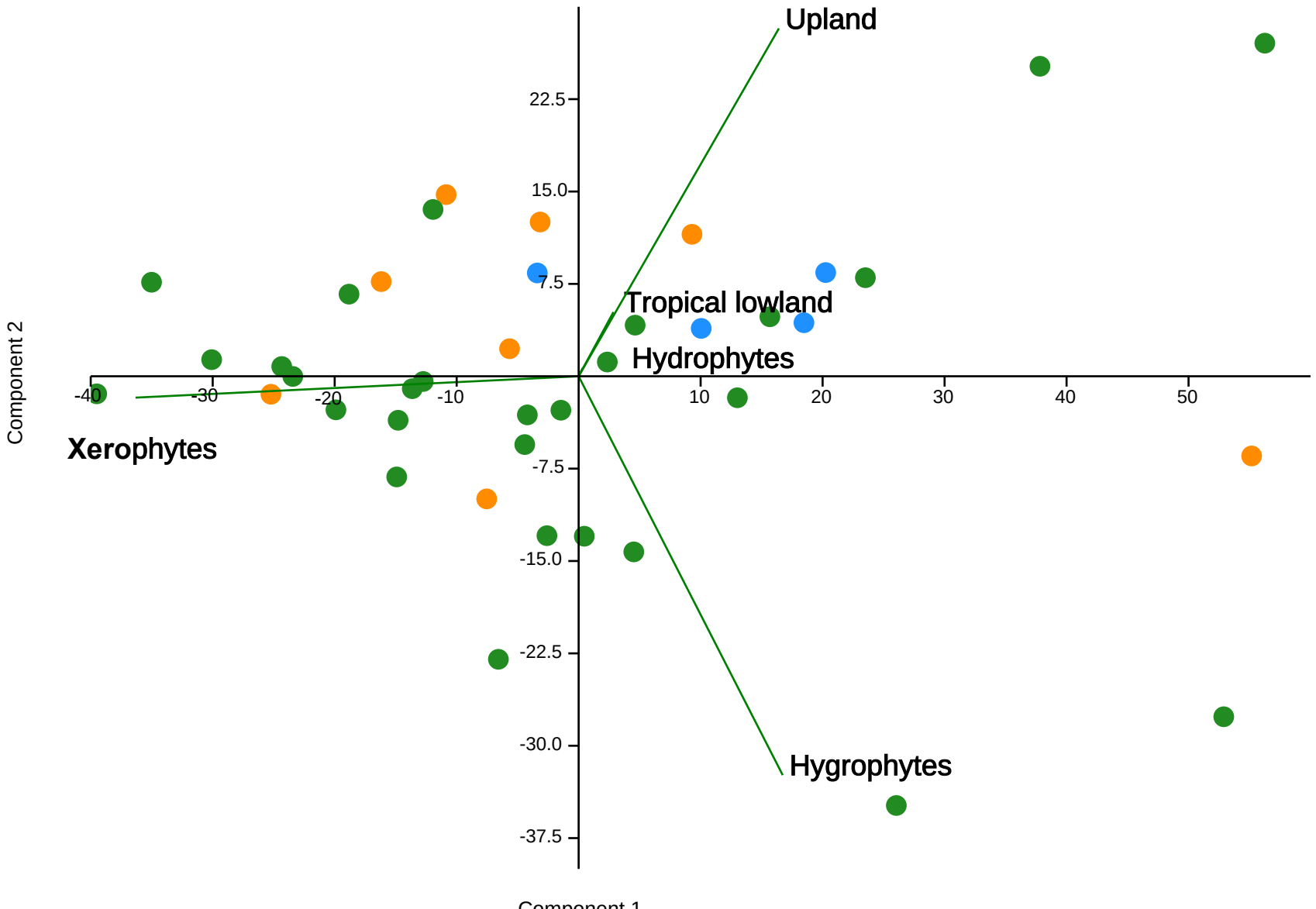


Figure 10. Principal component plot of bioclimatic groups for the pre-evaporitic phase (green dots, N = 28), evaporitic phase (orange dots, N = 8), and post-evaporitic phase (blue dots, N =4).

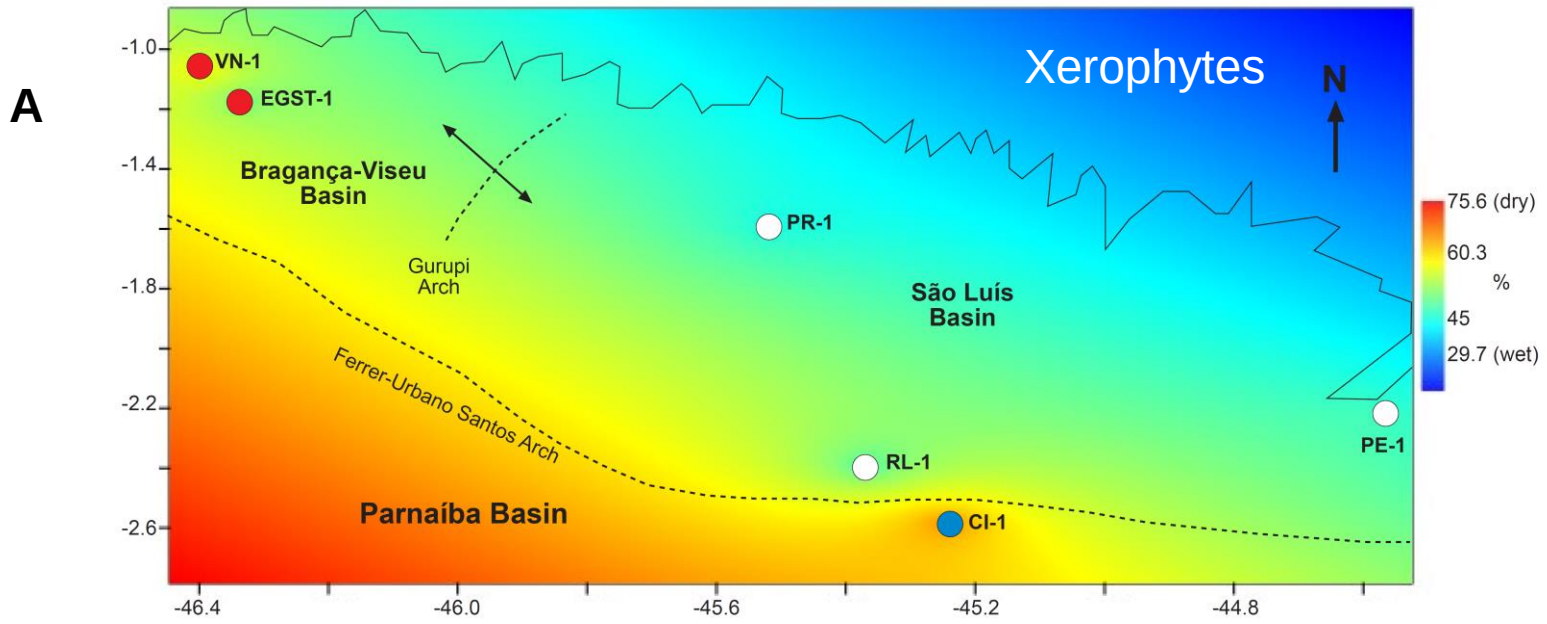


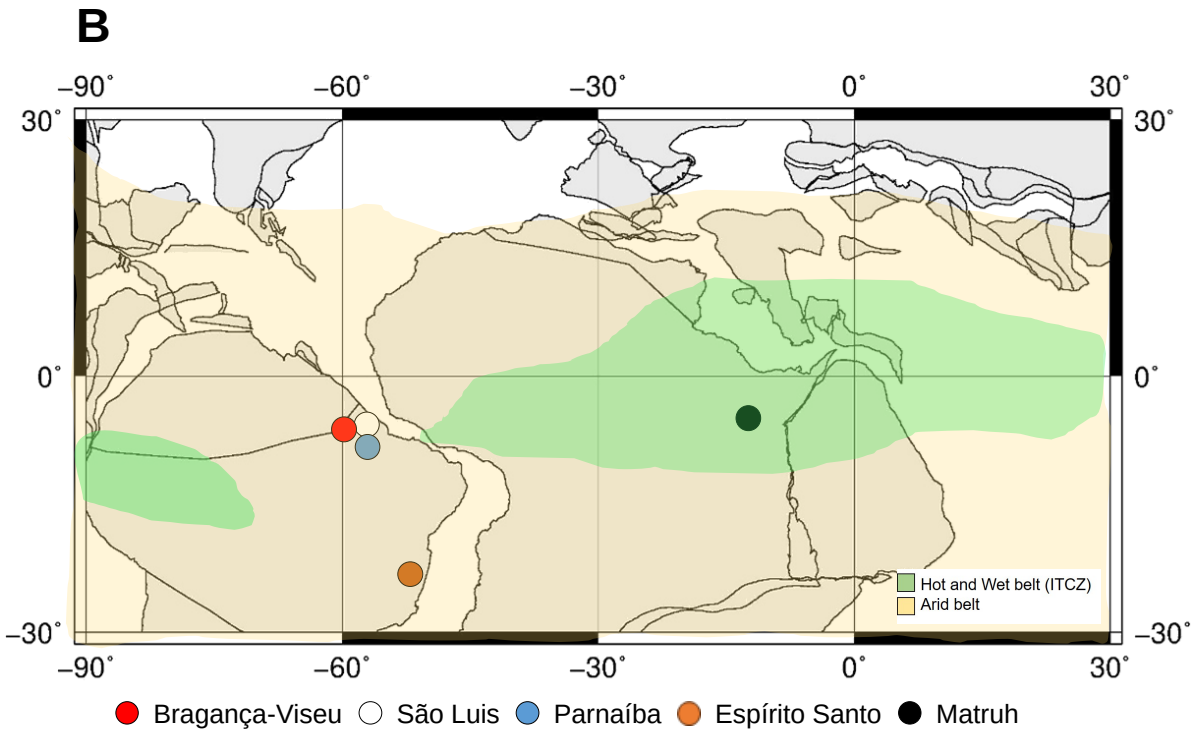


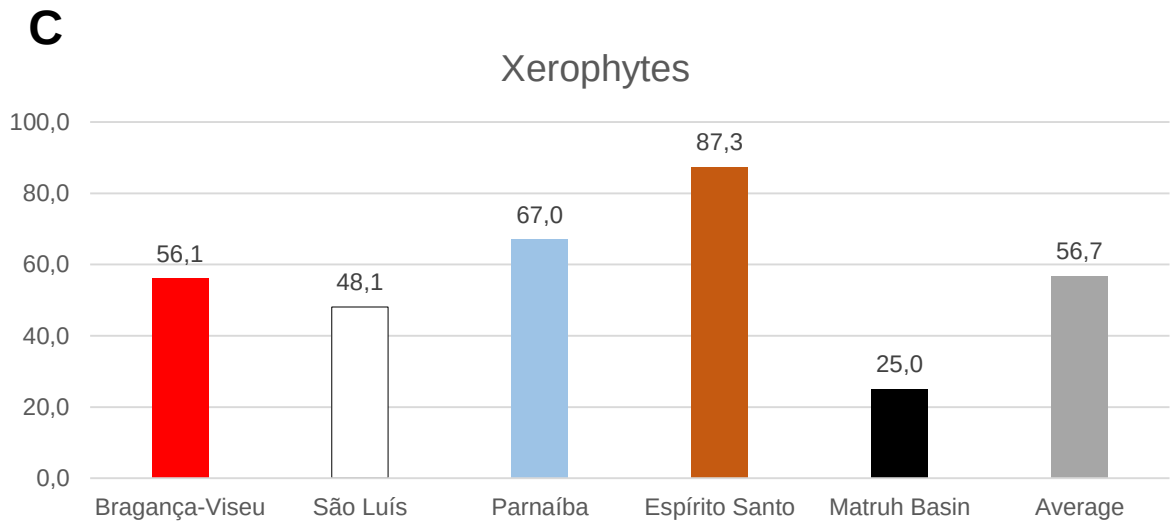


Figure 11. A) Late Aptian latitudinal distribution of the xerophyte bioclimatic group. B) Paleoclimatic belts of the late Aptian in South America (climatic belts modified from Scotese, 2016). Reconstruction map at 116 Ma modified from ODSN Plate Tectonic Reconstruction Service. C) Comparison of the bioclimatic group Xerophytes by basin. Data from the Mathru Basin (Dahab Formation) from Deaf et al. (2020).

Table 1. Localities, lithostratigraphy of the studied sections and lithologies of studied interval.

| Wells | Basins | Lithostratigraphy (Formation) | Interval (m) | Lat (S) | Long (W) | No. total core samples | Lithology of the studied interval |
|---|---|---|---|---|---|---|---|
| EGST-1 | Bragança-Vizeu | Bragança Fm. | 676-1872.1 | -01:17:55.229 | -46:34:55.683 | 8 | Sandstones, siltstones, conglomerates. |
| VN-1 | Bragança-Vizeu | Bragança Fm. | 1287.6-1317.69 | -01:06:48.216 | -46:40:35.673 | 4 | Sandstones. |
| PE-1 | São Luís | Codó Fm. | 1562-1776.8 | -02:22:09.725 | -44:57:28.505 | 4 | Sandstones, siltstones, calcarenites. |
| RL-1 | São Luís | Codó Fm. | 1157.3-1240.3 | -02:40:21.105 | -45:37:09.065 | 7 | Sandstones, siltstones, calcarenites, anhydrites. |
| PR-1 | São Luís | Codó Fm. | 1507.6-1513.1 | -01:59:59.070 | -45:52:58.477 | 4 | Sandstones, siltstones. |
| CI-1 | Parnaíba | Codó Fm. | 768-907.1 | -02:59:54.215 | -45:24:30.842 | 13 | Sandstones, siltstones, conglomerates, calcarenites, anhydrites |

Table 2. Plant groups, palynomorph taxa, botanical affinities and bioclimatic groups of the material studied.

| Plant Groups | Palynomorph taxa | Botanical affinities | Bioclimatic groups |
|---|---|---|---|
| Bryophytes | *Aequitriradites* | Hepaticae | Hygrophyte |
| | *Cingutriletes* | Sphagnaceae | Hygrophyte |
| | *Stereisporites* | Sphagnaceae | Hygrophyte |
| | *Triporoletes* | Ricciaceae | Hygrophyte |
| Ferns | *Appendicisporites* | Schizaeales (Anemiaceae?) | Hygrophyte |
| | *Biretisporites* | Osmundaceae | Hygrophyte |
| | *Cicatricosisporites* | Schizaeales (Anemiaceae?) | Hygrophyte |
| | *Crybelosporites* | Marsileaceae | Hydrophyte |
| | *Cyathidites* | Cyatheaceae-Dicksoniaceae | Upland flora |
| | *Deltoidospora* | Cyatheaceae-Dicksoniaceae | Upland flora |
| | *Distaltriangulisporites* | Schzaeales (Schizaeaceae?) | Hygrophyte |
| | *Foveotriletes* | Schzaeales (Schizaeaceae?) | Hygrophyte |
| | *Gleicheniidites* | Gleicheniaceae | Hygrophyte |
| | *Granulatisporites* | Pteridaceae | Hygrophyte |
| | *Klukisporites* | Schizaeales (Lygodiaceae?) | Hygrophyte |
| | *Matonisporites* | Matoniaceae | Upland flora |
| | *Paludites* | Marsileaceae | Hydrophyte |
| | *Reticulosporis* | Schzaeales (Schizaeaceae?) | Hygrophyte |
| | *Todisporites* | Osmundaceae | Hygrophyte |
| | *Undulatisporites* | Schzaeales (Schizaeaceae?) | Hygrophyte |
| | *Verrucosisporites* | Osmundaceae (?) | Hygrophyte |
| Lycophytes | *Antulsporites* | Selaginellaceae | Hygrophyte |
| | *Camarozonosporites* | Lycopodiaceae | Hygrophyte |
| | *Cingulatisporites* | Selaginellaceae | Hygrophyte |
| | *Densoisporites* | Selaginellaceae | Hygrophyte |
| | *Echinatisporites* | Selaginellaceae | Hygrophyte |
| | *Hamulatisporis* | Lycopodiaceae | Hygrophyte |
| | *Leptolepidites* | Lycopodiaceae | Hygrophyte |
| | *Lycopodiumsporites* | Lycopodiaceae | Hygrophyte |
| | *Perotrilites* | Selaginellaceae | Hygrophyte |
| | *Uvaesporites* | Selaginellaceae | Hygrophyte |
| Gymnosperms | *Araucariacites* | Araucariaceae | Upland flora |
| | *Balmeiopsis* | Araucariacites | Upland flora |
| | *Bennettitaepollenites* | Cycadaceae | Tropical lowland flora |
| | *Callialasporites* | Araucariacites/Podocarpaceae | Upland flora |
| | *Cavamonocolpites* | Cycadaceae | Tropical lowland flora |
| | *Cedripites* | Pinaceae | Upland flora |
| | *Cingulatipollenites* | Araucariaceae | Upland flora |
| | *Classopollis* | Cheirolepidiaceae | Xerophytes |
| | *Complicatisaccus* | Coniferae i. sedis | Upland flora |
| | *Cycadopites* | Cycadaceae | Tropical lowland flora |

| | | | |
|---|---|---|---|
| | *Elateropollenites* | Gnetales (Gnetaceae?) | Xerophytes |
| | *Equisetosporites* | Gnetales (Ephedraceae?) | Xerophytes |
| | *Eucommiidites* | Erdtmanithecales | Xerophytes |
| | *Exesipollenites* | Cupressaceae | Upland flora |
| | *Gnetaceaepollenites* | Gnetales (Gnetaceae?) | Xerophytes |
| | *Inaperturopollenites* | Cupressaceae | Upland flora |
| | *Regalipollenites* | Gnetales (Ephedraceae?) | Xerophytes |
| | *Rugubivesiculites* | Podocarpaceae | Upland flora |
| | *Sergipea* | Gnetales | Xerophytes |
| | *Singhia* | Gnetales (Ephedraceae?) | Xerophytes |
| | *Spheripollenites* | Cupressaceae | Upland flora |
| | *Steevesipollenites* | Gnetales (Gnetaceae?) | Xerophytes |
| | *Uesuguipollenites* | Cupressaceae | Upland flora |
| | *Vitreisporites* | Caytoniaceae | Upland flora |
| Angiosperms | *Afropollis* | ? | Tropical lowland flora |
| | *Arecipites* | Monocots (Arecaceae?) | Tropical lowland flora |
| | *Brenneripollis* | Chloranthaceae | Tropical lowland flora |
| | *Clavatipollenites* | Chloranthaceae | Tropical lowland flora |
| | *Cretacaeiporites* | Trimeniaceae? | Tropical lowland flora |
| | *Dejaxpollenites* | ? | Tropical lowland flora |
| | *Monocolpopollenites* | Monocots (Arecaceae?) | Tropical lowland flora |
| | *Psiladicolpites* | Monocots (Liliaceae?) | Tropical lowland flora |
| | *Retimonocolpites* | Monocots (Arecaceae?) | Tropical lowland flora |
| | *Retiquadricolpites* | ? | Tropical lowland flora |
| | *Rousea* | Eudicots (Flacourtiaceae?) | Tropical lowland flora |
| | *Stellatopolis* | ? | Tropical lowland flora |
| | *Tricolpites* | Eudicots | Tropical lowland flora |
| | *Trisectoris* | Illiciaceae | Tropical lowland flora |

Table 3. Description of the bioclimatic groups and their main representatives.

| Bioclimatic groups | Main representatives (sporomoph genera) | Remarks |
|---|---|---|
| Hydrophytes | *Crybellosporites* | Hydrophytes represent aquatic plants that live with a portion of their vegetative parts permanently immersed in water. |
| Hygrophytes | *Cicatricosisporites* | Hygrophyte plants depend on water to reproduce and are therefore generally associated with moist conditions and rarely reported from arid environments. |
| Tropical lowland flora | *Afropollis* | The tropical lowland flora is composed by families related to more humid conditions in lowland areas. All angiosperm genera and morphotypes are included in this flora |
| Upland flora | *Araucariacites, Caliallasporites* | Families assigned to thermophilic, large conifers, formed forests in the highlands from 200 to 1800 m. |
| Xerophytes | *Classopollis, Gnetaceaepollenites* | The group is adapted to xeric or water-stressed environments and therefore associated with arid climates. |

Table 4. Average abundance of bioclimatic groups, diversity (H') and Fs/X ratio of the studied wells.

| Basins | Wells | Hydrophytes | Hygrophytes | Tropical lowland flora | Upland flora | Xerophytes | Fs/X | H' |
|---|---|---|---|---|---|---|---|---|
| Bragança-Viseu | EGST-1 | 0.9 | 24.9 | 5.5 | 16.6 | 52.1 | 0.38 | 2.1 |
| Bragança-Viseu | VN-1 | 0.2 | 28.4 | 1.6 | 9.7 | 60.2 | 0.31 | 1.6 |
| São Luís | PR-1 | 1.0 | 14.3 | 20.4 | 18.0 | 46.3 | 0.25 | 2.1 |
| São Luís | PE-1 | 0.1 | 16.8 | 8.5 | 26.0 | 48.6 | 0.28 | 2.2 |
| São Luís | RL-1 | 1.0 | 15.8 | 12.0 | 7.8 | 63.4 | 0.24 | 1.9 |
| Parnaíba | CI-1 | 0.7 | 11.4 | 6.0 | 15.9 | 63.6 | 0.19 | 2.0 |
| *General average* | | *0.7* | *18.6* | *9.0* | *15.7* | *55.7* | *0.28* | *2.0* |

Table 5. Average abundance of bioclimatic groups, diversity, Fs/X and marine elements of the paleoclimatic phases for the Bragança-Viseu, São Luís and Parnaíba basins. No marine elements.

| Paleoclimatic phases | Hygrophytes | Hydrophytes | Tropical lowland flora | Upland flora | Xerophytes | Diversity (H') | Fs/X | IndVal |
|---|---|---|---|---|---|---|---|---|
| Pre-evaporitic | 18.8 | 0.7 | 5.6 | 14.1 | 60.7 | 2.0 | 0.3 | *Deltoidospora* sp. (80.6%) |
| Evaporitic | 10.0 | 1.0 | 16.0 | 5.0 | 67.9 | 2.2 | 0.1 | *Afropollis* spp. (79.3%) |
| Post-evaporitic | 15.5 | 0.6 | 14.4 | 22.0 | 47.4 | 2.1 | 0.3 | *Deltoidospora* sp. (86.2%) |
| *General average* | *14.8* | *0.8* | *12.0* | *13.7* | *58.7* | *2.1* | *0.2* | |

Appendix 1. Eleven plates with the most relevant palynomorphs recorded in the studied wells.

**PLATE 1**

A. *Stereisporites* sp. Pflug, 1953 (RL-1).

B. *Todisporites* sp. Couper, 1958 (RL-1).

C. *Deltoidospora diaphana* Wilson & Webster, 1946 (EGST-1).

D-E. *Deltoidospora minor* (Couper 1953) Pocock 1970ª (CI-1).

F. *Cyathidites* sp. Couper, 1953 (CI-1).

G. *Cyathidites minor* Couper, 1953 (CI-1).

H. *Biretisporites* sp. Delcourt & Sprumont, 1955 emend. Delcourt, Dettmann & Hughes, 1963 (CI-1).

I. *Biretisporites pontoniaei* Delcourt & Sprumont, 1955 (RL-1).

J. *Undulatisporites* sp.? Thomson & Pflug, 1953 (CI-1).

K. *Granulatosporites* sp. Ibrahim, 1933 (CI-1).

L. *Verrucosisporites* sp. Ibrahim, 1933 *emend.* Potonié & Kremp, 1955 (CI-1).

**PLATE 2**

A. *Leptolepidites psarosus* Norris, 1966 (CI-1).

B. *Leptolepidites verrucatus* Couper, 1953 (CI-1).

C-D. *Uvaesporites* sp. Doring, 1965 (CI-1).

E. *Apiculatisporis* sp. Potonié & Kremp, 1954 (CI-1).

F. *Echinatisporis* sp. Krtuzsch, 1959 (CI-1).

G. *Hamulatisporis* sp. Krtuzsch, 1959 (RL-1).

H. *Cicatricosisporites* sp. Potonié & Gelletch, 1933 (EGST-1).

I. *Cicatricosisporites avnimelechi* Horowitz, 1970 (CI-1).

J-K. *Cicatricosisporites brevilaesuratus* Couper, 1958 (EGST-1).

L. *Cicatricosisporites cf. Cicatricosisporites?* sp.5 Duarte, 2011 (EGST-1).

**PLATE 3**

A - B. *Lycopodiumsporites* sp. Thiegart, 1938 (RL-1).

C. *Klukisporites variegatus* Couper, 1958 (CI-1).

D. *Klukisporites* sp. Couper, 1958 (RL-1).

E. *Klukisporites foveolatus* Pocock, 1964 (EGST-1).

F. *Klukisporites pseudoreticulatus* Couper, 1958 (CI-1).

G. *Foveotriletes* sp. Hammen, 1956 (CI-1).

H. *Gleicheniidites senonicus* Ross, 1949 (PR-1).

I. *Camarozonaesporites* sp. Pant, 1954 *ex.* Potonié, 1956 *emend.* Klaus, 1960 (VN-1).

J. *Antulsporites* sp. Archangelsky & Gamerro, 1966 (CI-1).

K. *Cingulatisporites verrucatus* Regali, Uesugui & Santos, 1974 (PE-1)

L. *Distaltriangulisporites* sp. Singh, 1971 (RL-1).

M. *Cingutriletes* sp. Pierce, 196 (PR-1).

**PLATE 4**

A. *Matonisporites silvai* Lima, 1978 (PR-1).

B-C. *Appendicisporites* sp. Weiland & Krieger, 1953; (PR-1).

D. *Aequitriradites* sp. Delcourt & Sprumont, 1955 *emend.* Dettmann, 1963 (RL-1).

E. *Perotrilites* sp. Erdtman, 1947 *ex.* Couper, 1953 (RL-1).

F. *Crybelosporites pannuceus* Brenner,1963 *emend.*Srivastava, 1975 (RL-1)

G. *Paludites mameolatus* Lima, 1978 (PR-1).

H. *Densoisporites* sp. Weyland & Krieger, 1953 (EGST-1).

I. *Triporoletes* sp. Mtchedlishvili, 1960 (RL-1).

J. *Reticulosporis* sp. Krutzsch, 1959 (PR-1).

K. *Reticulosporis foveolatus* Krutzsch, 1959 (EGST-1).

L. *Callialasporites trilobatus* Dev, 1961 (CI-1).

**PLATE 5**

A. *Callialasporites dampieri* Dev, 1961 (CI-1).

B. *Complicatisaccus cearensis* Regali, 1989c (PR-1).

C. *Cedripites* sp. Wodehouse, 1933 (CI-1).

D. *Vitreisporites pustulosus* Regali, 1987 (PR-001-MA); (PE-1).

E. *Vitreisporites microsaccus* Jersey, 1964 (PR-1).

F. *Vitreisporites pallidus* Nilsson, 1958 (PR-1).

G. *Rugubivesiculites bahiasulensis* Pierce, 1961 (RL-1).

H. *Inaperturopollenites* sp. (Pflug, 1952 ex. Thomson e Pflug, 1953, Potonié, 1958) Potonié, 1966 (RL-1).

I. *Araucariacites* sp. Cookson, 1947 ex Couper, 1953 (CI-1).

J. *Araucariacites australis* Cookson, 1947 (CI-1).

K. *Araucariacites limbatus (*Balme) Habib, 1957 (EGST-1).

L. *Araucariacites pergranulatus* Volkheimer, 1968 (EGST-1).

**PLATE 6**

A. *Araucariacites* sp. S. CI. 265 A Jardiné & Magloire, 1965 (EGST-1).

B. *Balmeiopsis* sp.*?* Archangelsky, 1977 (PE-1).

C. *Balmeiopsis limbatus* Archangelsky, 1977 (EGST-1).

D. *Cingulatipollenites* sp.*?* Saad & Ghazaly, 1976 (PE-1).

E. *Cingulatipollenites aegyptiaca* Saad & Ghazaly, 1976 (EGST-1)

F. *Spheripollenites* sp. Couper, 1958 (RL-1).

G. *Spheripollenites scabratus* Couper, 1958 (EGST-1).

H. *Sergipea variverrucata* Regali, Uesugui & Santos, 1974 *emend.* Regali, 1987 (PR-1).

I. *Sergipea simplex* Regali, 1987 (PE-1).

J. *Uesuguipollenites callosus* Dino, 1992 (RL-1).

K. *Classopollis classoides* Pflug, 1953 (CI-1).

L. *Classopollis brasiliensis* Herngreen, 1973 (PE-1).

**PLATE 7**

A. *Equisetosporites aff. elegans* Lima, 1978 (CI-1).

B. *Equisetosporites dudarensis* (Deák, 1964) Lima, 1980 (CI-1).

C. *Equisetosporites ambuguus* Hedlund, 1966 (RL-1).

D. *Equisetosporites consinnus* Singh, 1964 (PR-1).

E. *Equisetosporites leptomatus* Lima, 1978 (CI-1).

F. *Equisetosporites luridus* Lima, 1978 (CI-1).

G. *Equisetosporites lanceolatus* Lima, 1978 (CI-1).

H. *Equisetosporites aff. leptomatus* Lima, 1978 (CI-1).

I. *Elateropollenites bicornis* Regali, 1989e (EGST-1).

J. *Elateropollenites dissimilis* Regali, 1989e (EGST-1).

K. *Classopollis intrareticulatus* Volkheimer, 1972 (PR-1).

L. *Equisetosporites aff. luridus* Lima, 1978 (RL-1).

**PLATE 8**

A. *Equisetosporites maculosus* Dino, 1992 (CI-1).

B. *Equisetosporites minuticostatus* Lima, 1978 (PR-1).

C. *Equisetosporites aff. minuticostatus* Lima, 1978 (CI-1).

D. *Equisetosporites ovatus* (Pierce) Singh, 1961 (CI-1).

E. *Gnetaceaepollenites* sp. Thiegart, 1938 (CI-1).

F. *Gnetaceaepollenites consisus* Regali, 1989c (CI-1).

G. *Gnetaceaepollenites jansonii* Pocock, 1964 (CI-1).

H. *Gnetaceaepollenites uesuguii* Lima, 1978 (CI-1).

I. *Gnetaceaepollenites undulatus* Regali, Uesugui & Santos, 1974 (RL-1).

J. *Steevesipollenites* sp. Stover, 1964 (CI-1)..

K. *Singhia* sp. Srivastava, 1968 (PR-1).

L. *Singhia punctata* Lima, 1978 (EGST-1)

**PLATE 9**

A. *Regalipollenites* sp. Lima, 1978 (PR-1).

B. *Eucommiidites* sp. (Erdtman, 1948) Hugues, 1961 (CI-1).

C. *Eucommiidites troedssonii* (Erdtman, 1948) Hugues, 1961 (RL-1).

D. *Arecipites microfoveolatus* Ibrahim, 2002 (CI-1)

E. *Cycadopites* sp. Wilson e Webster, 1946 (PE-1).

F. *Dejaxpollenites foveoreticulatus* Dino, 1992 (EGST-1)

G. *Bennettitaepollenites* sp. Thiegart, 1949 (CI-1)

H. *Cavamonocolpites* sp. Lima, 1978 (RL-1).

I. *Cavamonocolpites* sp.1 Dino, 1992 (CI-1).

J. *Clavatipollenites* sp. Couper, 1958 (EGST-1).

K. *Clavatipollenites huguesi* Couper, 1958 (PE-1).

L. *Stellatopollis* sp. Doyle, Van Campo e Lugardon, 1975 (VN-1).

**PLATE 10**

A. *Retimonocolpites* sp. Pierce, 1961 (PR-1).

B. *Monocolpopollenites* sp. Thomsom & Pflug, 1953 *emend.* Nichols, Ames & Traverse, 1973 (CI-1).

C. *Brenneripollis reticulatus* Júhasz & Góczan, 1985 (PE-1).

D. *Afropollis jardinus* Doyle, Jardiné & Doeren Kamp, 1982 (CI-1).

E. *Afropollis aff. jardinus* Doyle, Jardiné & Doeren Kamp, 1982 (PR-1).

F. *Psiladicolpites papillatus ?* Regali, 1989c (EGST-1).

G. *Tricolpites* sp. Cookson, 1947 *ex* Couper, 1953 (EGST-1).

H. *Rousea* sp. Srivastava, 1969 (PR-1).

I. *Rousea georgensis* (Brenner, 1963) Dettmann, 1973 (PR-1).

J. *Trisectoris reticulatus* (Regali, Uesugui & Santos, 1974b) Heimhofer & Hochuli, 2010 (EGST-1).

K. *Retiquadricolpites* sp. Regali, 1989 (CI-1).

L. *Exesipollenites tumulus* Balme, 1957 (PR-1).

**PLATE 11**

A. *Cretacaeiporites* sp.*?* Herngreen, 1973 (RL-1).

B. *Schizosporis* sp. Cookson & Dettmann, 1959 (PE-1).

C. *Schizosporis parvus* Cookson & Dettmann, 1959 (RL-1).

D. *Schizosporis spriggi* Cookson & Dettmann, 1959 (EGST-1).

E. Acritarch Evitt 1963 (CI-1).

F. *Cymatiosphera ?* Wetzel, 1933 (CI-1).

G. *Duvernaysphaera* sp. (Staplin, 1961) Deunff, 1964 (CI-1).

H. *Maranhites* sp. Brito, 1965 *emend*. González, 2009 (CI-1).

I. *Tasmanites* sp. Newton, 1875 *emend*. Schopf, Wilson & Bentall, 1944 (CI-1).

J. *Scylaspora* sp. Burgess & Richardson, 1995 (EGST-1).

K. *Raistrickia* sp.? Schopf *etal.*1944 *emend.* Potonié & Kremp, 1954 (VN-1).

L. *Chomotriletes* sp. Naumova, 1937 (VN-1).

PLATE 1


A
10 µm

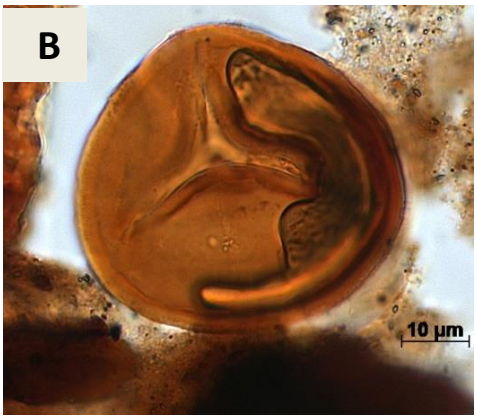
B
10 µm

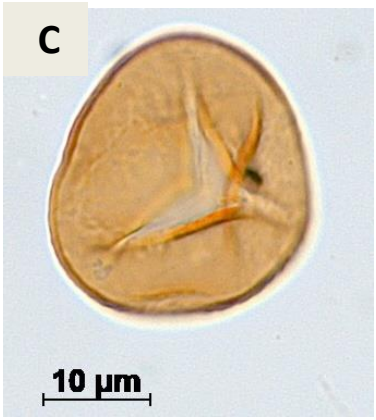
C
10 µm

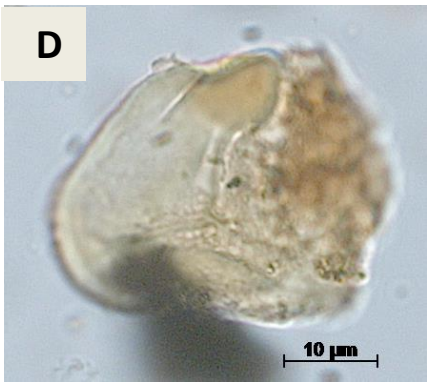
D
10 µm


E
10 µm

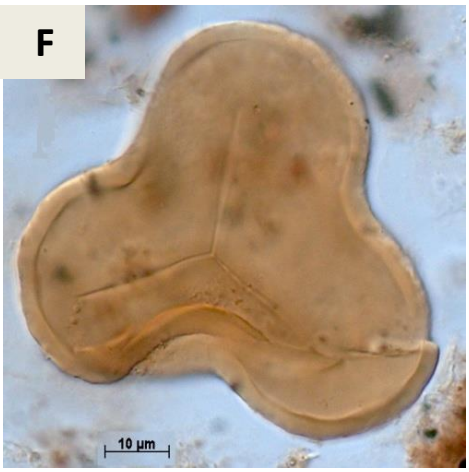
F
10 µm

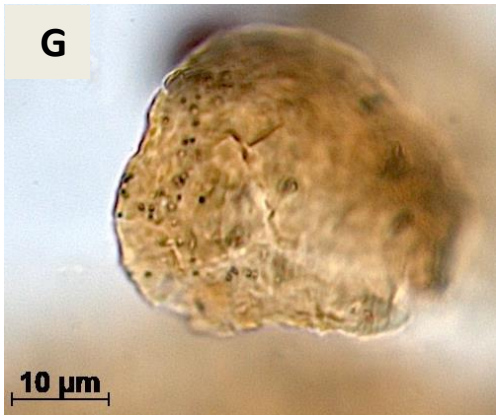
G
10 µm


H
10 µm


I
10 µm


J
10 µm

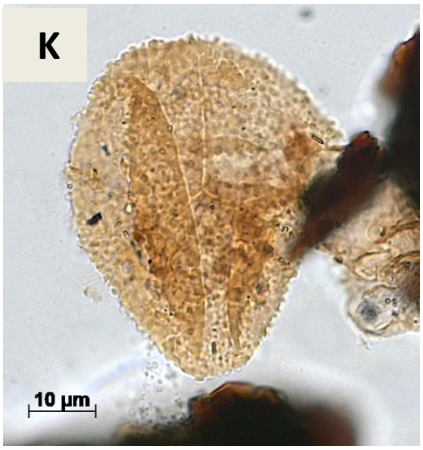
K
10 µm


L
10 µm

PLATE 2

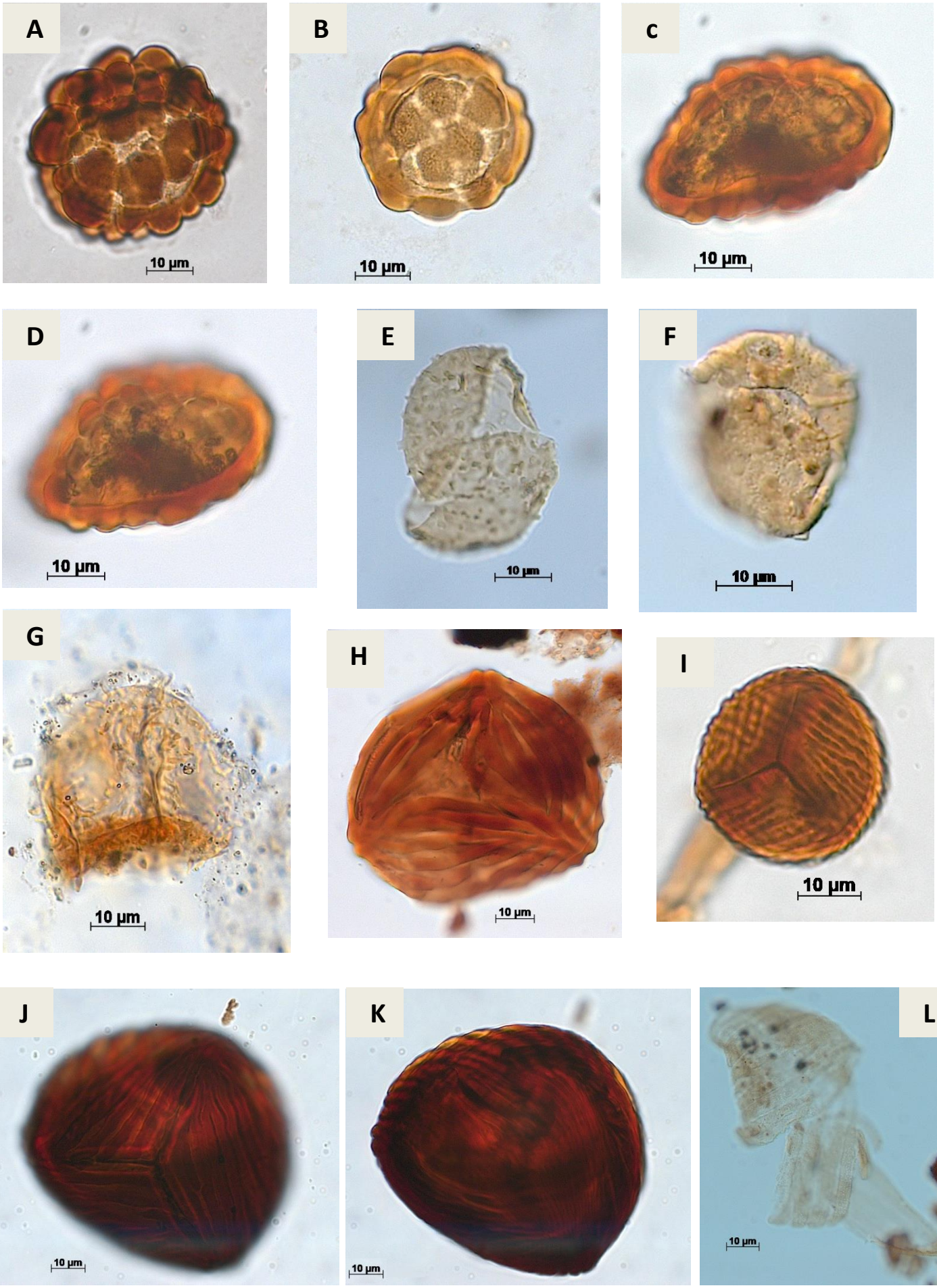
A
10 µm
B
10 µm
c
10 µm
D
10 µm
E
10 µm
F
10 µm
G
10 µm
H
10 µm
I
10 µm
J
10 µm
K
10 µm
L
10 µm

**PLATE 3**

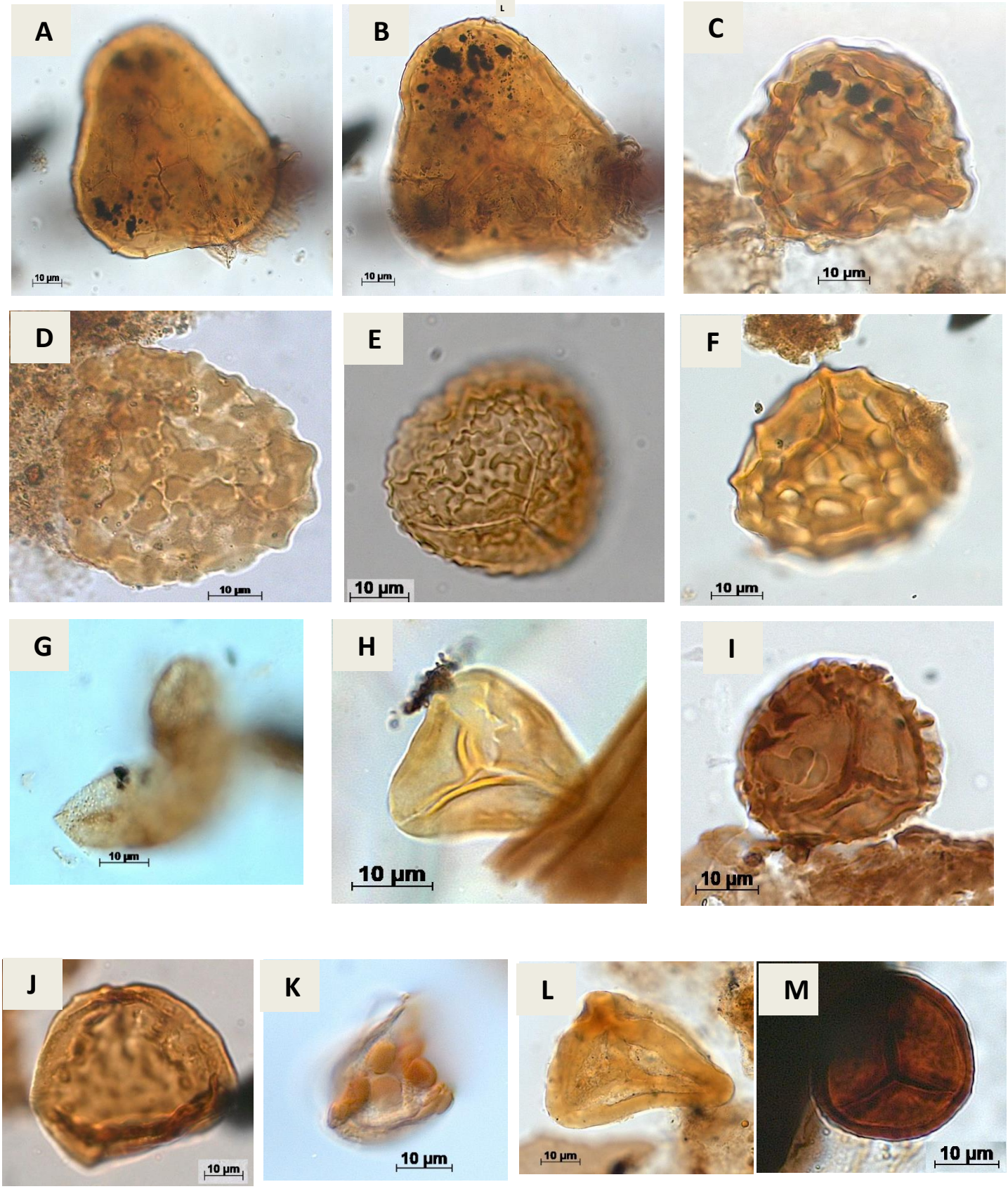
A
10 µm
B
10 µm
C
10 µm
D
10 µm
E
10 µm
F
10 µm
G
10 µm
H
10 µm
I
10 µm
J
10 µm
K
10 µm
L
10 µm
M
10 µm

**PLATE 4**

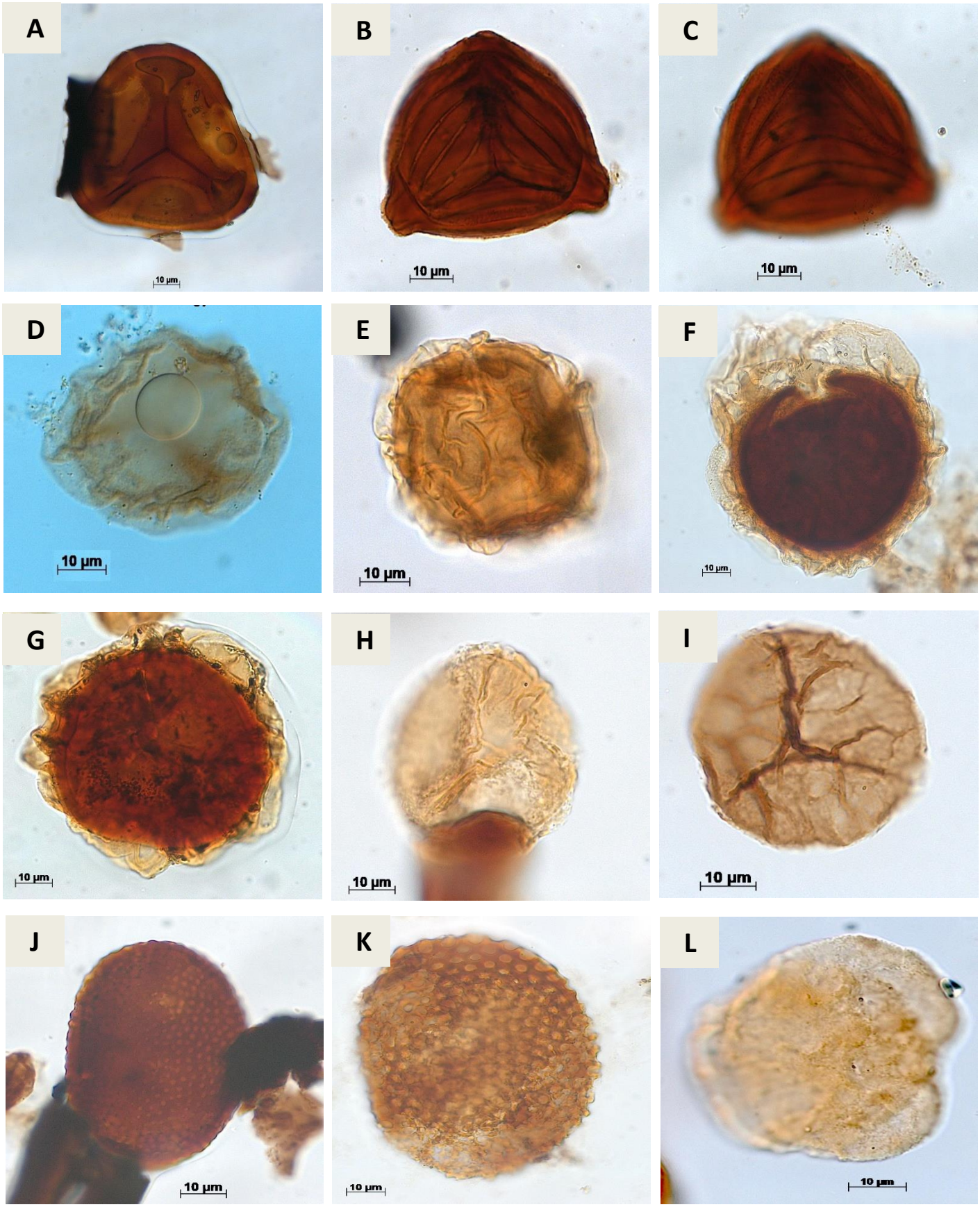

PLATE 5

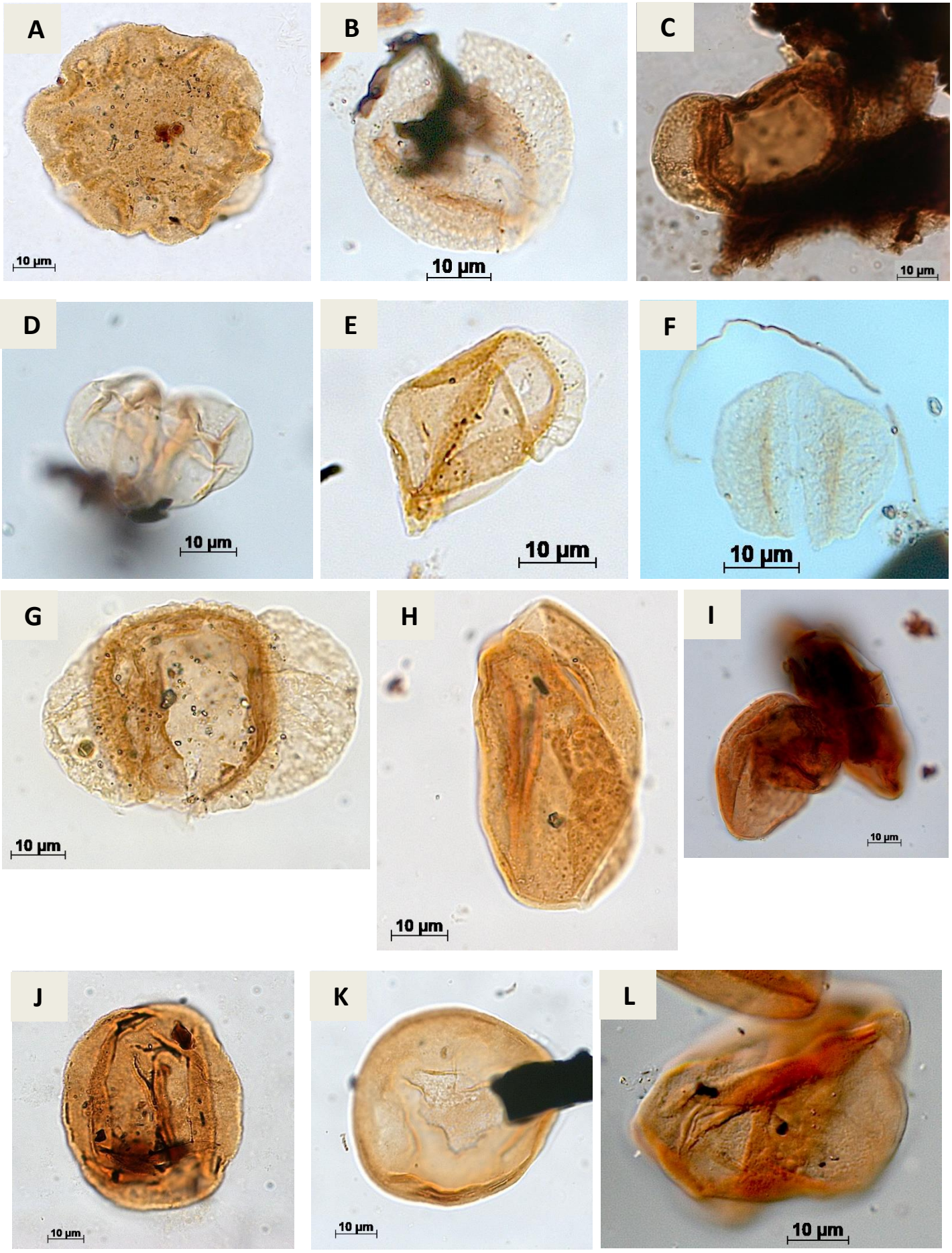
A
10 µm
B
10 µm
C
10 µm
D
10 µm
E
10 µm
F
10 µm
G
10 µm
H
10 µm
I
10 µm
J
10 µm
K
10 µm
L
10 µm

PLATE 6

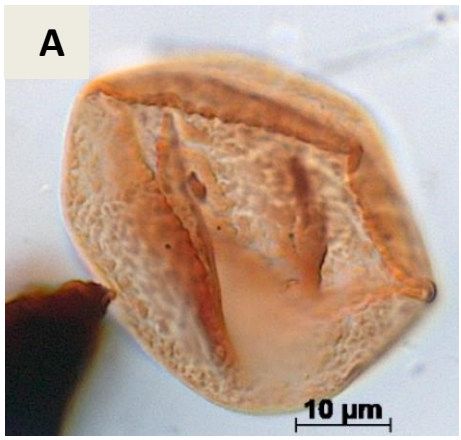
A
10 µm


B
10 µm


C
10 µm

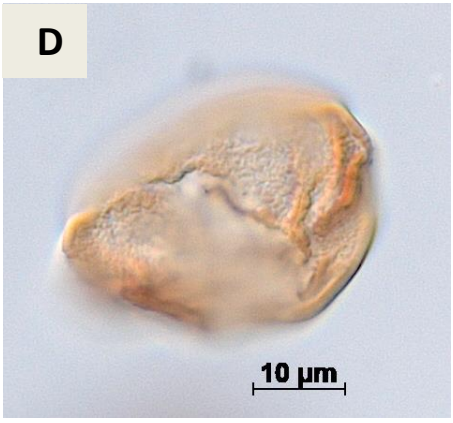
D
10 µm

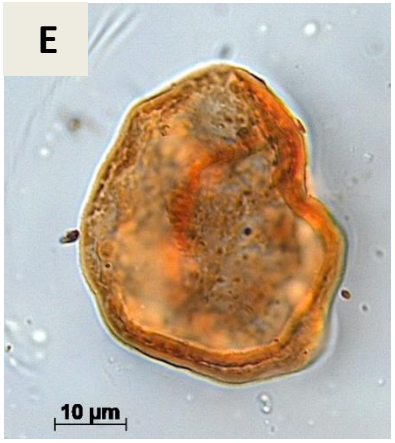
E
10 µm


F
10 µm


G
10 µm


H
10 µm

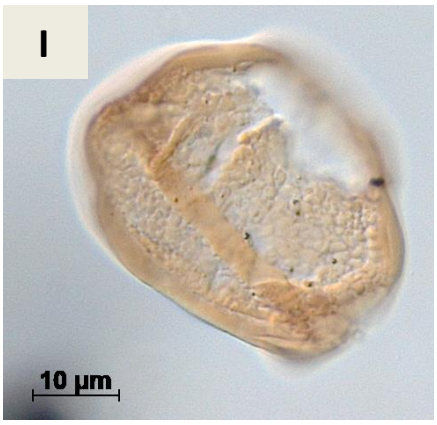
I
10 µm


J
10 µm


K
10 µm


L
10 µm

**PLATE 7**


A
10 µm


B
10 µm

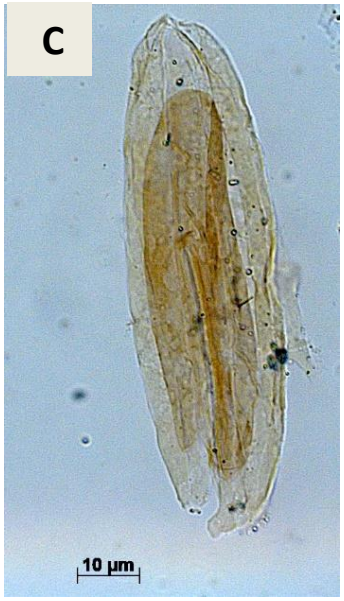
C
10 µm


D
10 µm


E
10 µm


F
10 µm


G
10 µm


H
10 µm

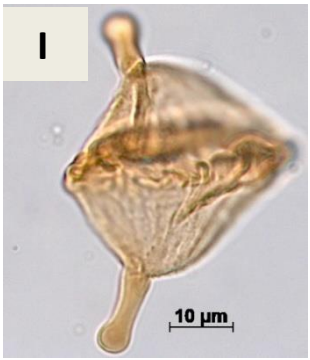
I
10 µm

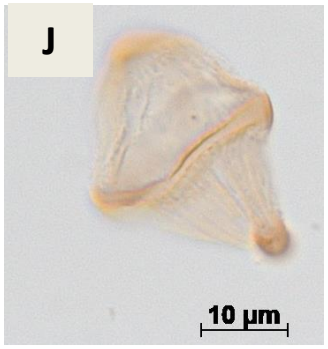
J
10 µm

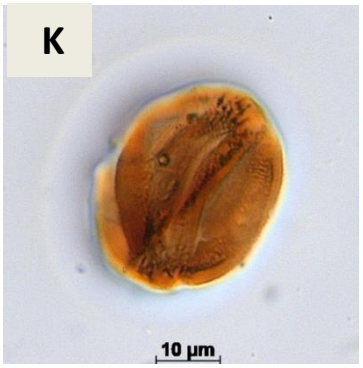
K
10 µm

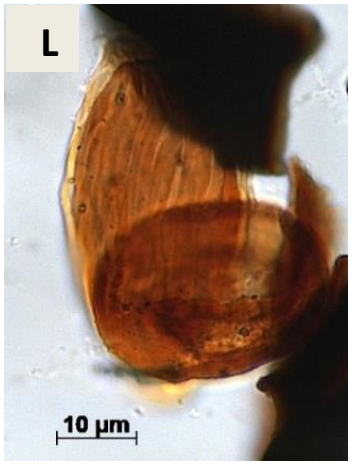
L
10 µm

**PLATE 8**

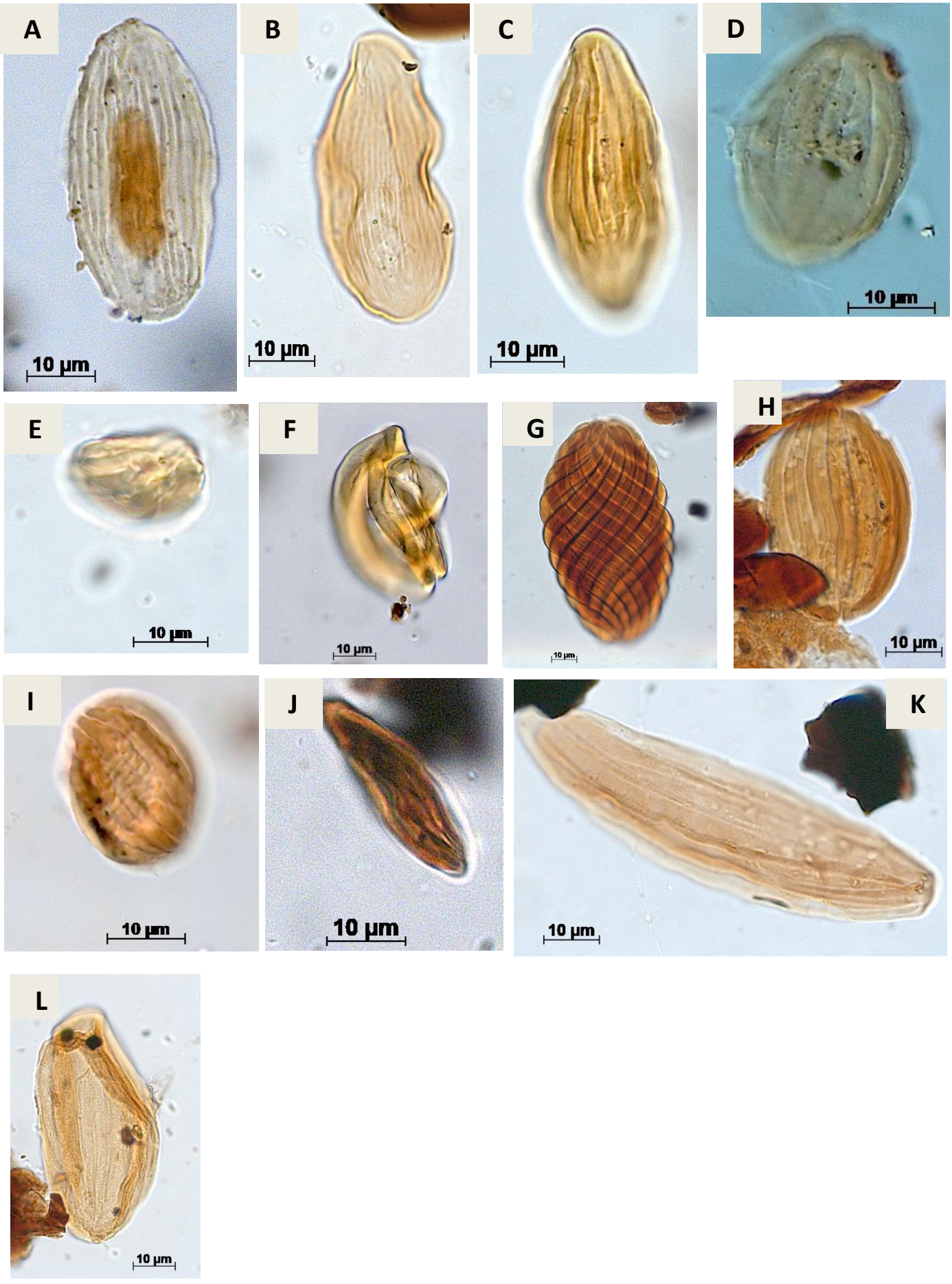
A
10 µm
B
10 µm
C
10 µm
D
10 µm
E
10 µm
F
10 µm
G
10 µm
H
10 µm
I
10 µm
J
10 µm
K
10 µm
L
10 µm

PLATE 9


A
10 µm


B
10 µm

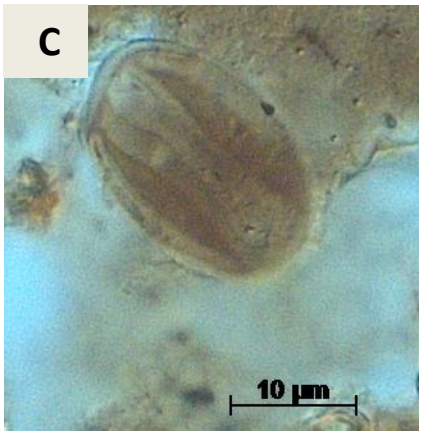
C
10 µm

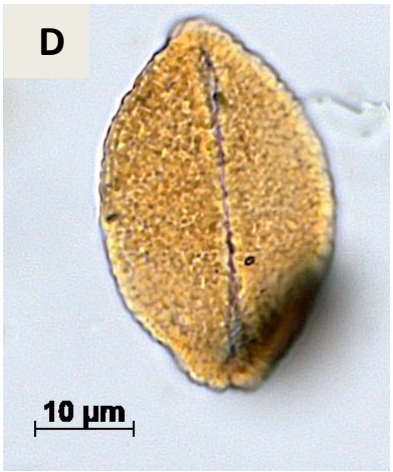
D
10 µm

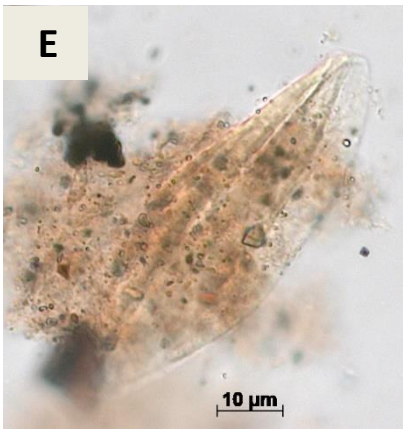
E
10 µm

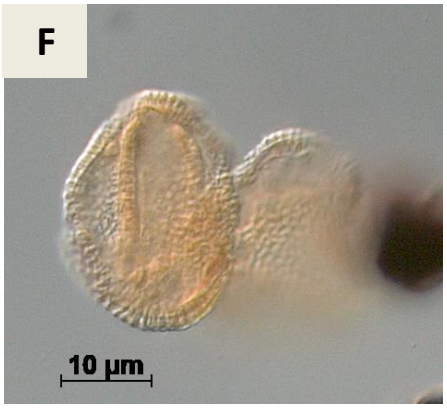
F
10 µm


G
10 µm

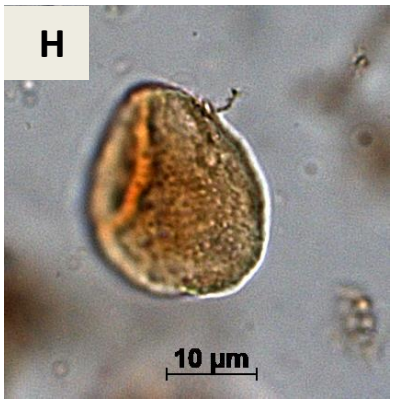
H
10 µm

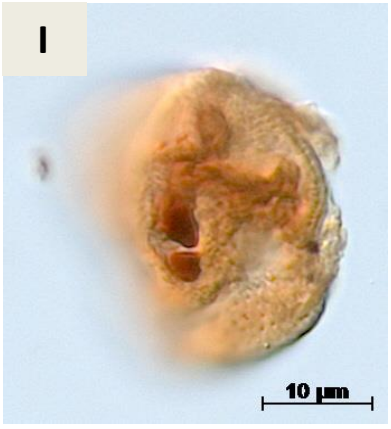
I
10 µm

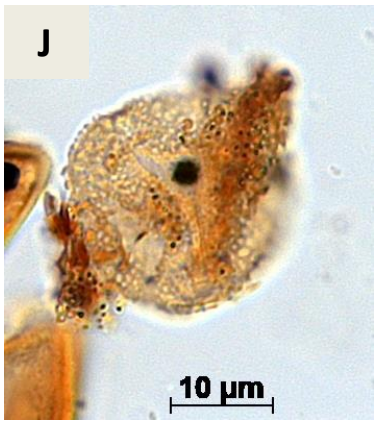
J
10 µm

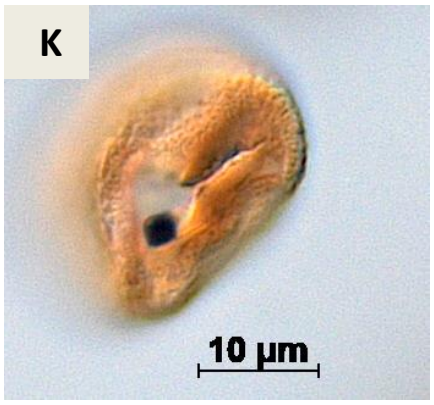
K
10 µm

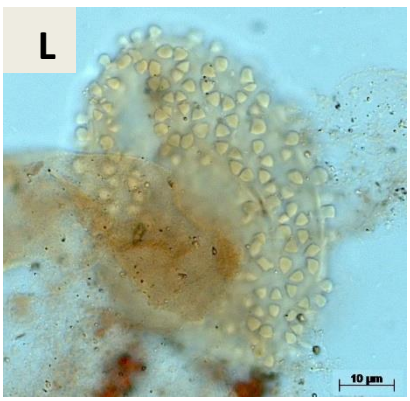
L
10 µm

**PLATE 10**

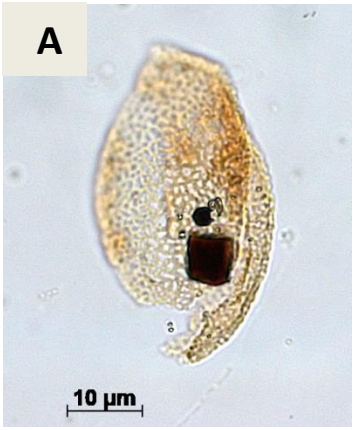
A
10 µm

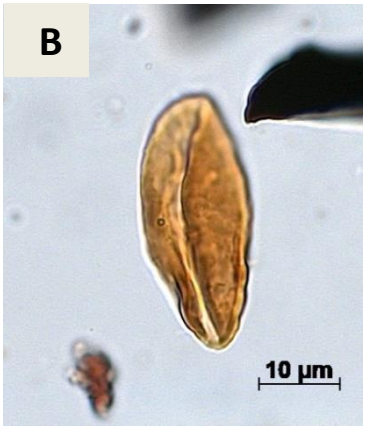
B
10 µm

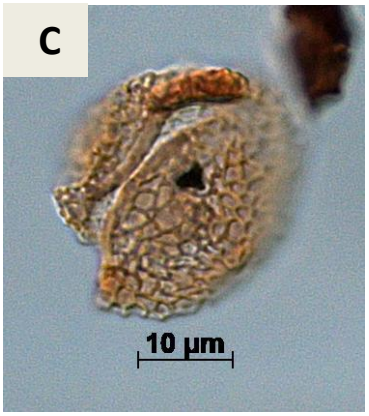
C
10 µm

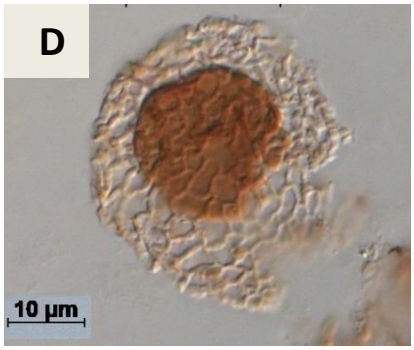
D
10 µm

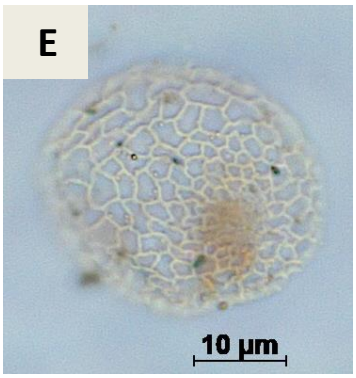
E
10 µm


F
10 µm

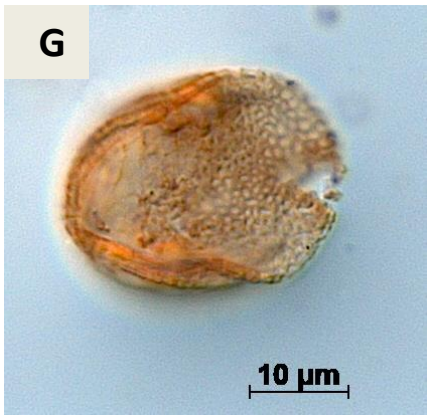
G
10 µm

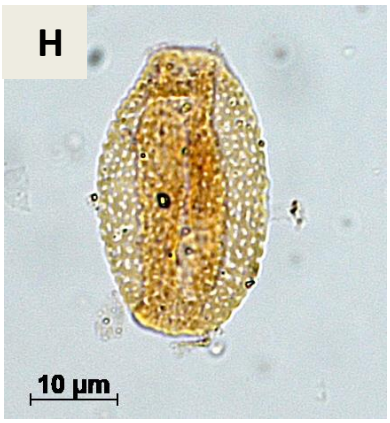
H
10 µm

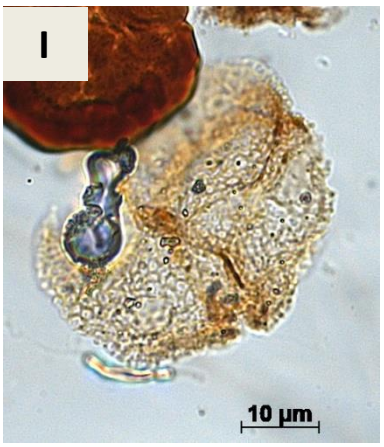
I
10 µm

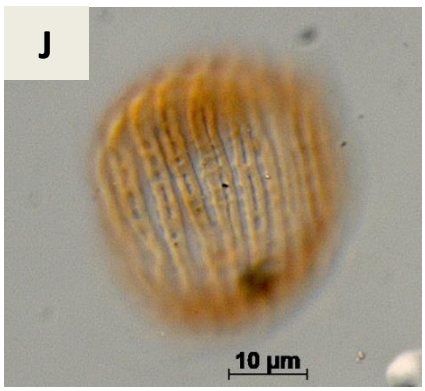
J
10 µm

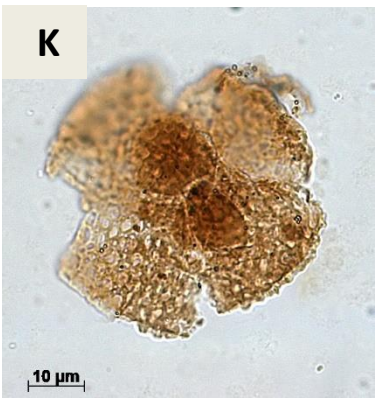
K
10 µm


L
10 µm

PLATE 11

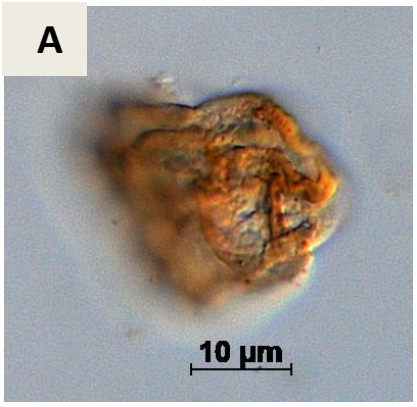
A
10 µm

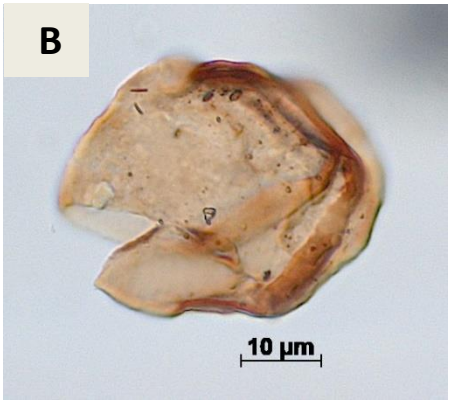
B
10 µm


C
20 µm


D
10 µm

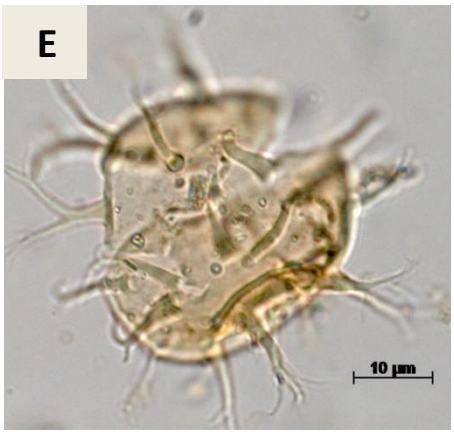
E
10 µm

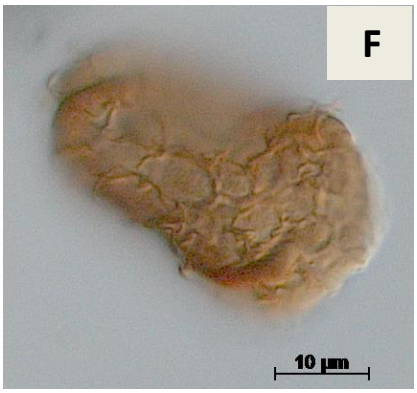
F
10 µm


G
10 µm

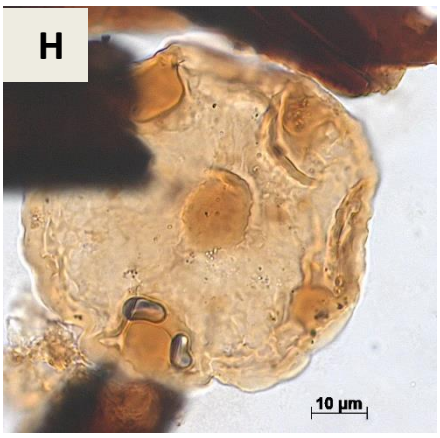
H
10 µm

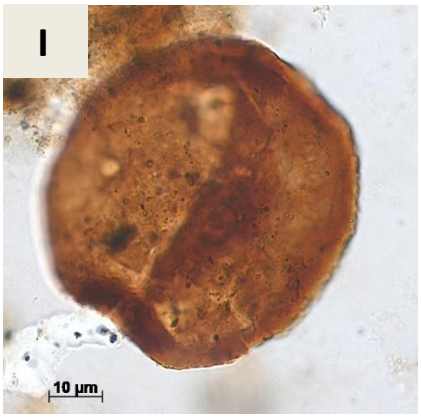
I
10 µm

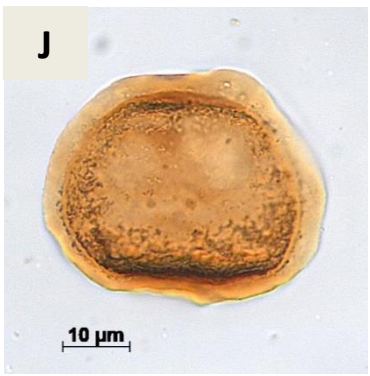
J
10 µm


K
10 µm


L
10 µm

Appendix 2. Bioclimatic groups (percentages) of studied wells. Legend: HG= hygrophytes; HD= hydrophytes; TLF= tropical lowland flora; UF= upland flora; XP= xerophytes; H'= diversity; Fs/X= fern spores/xerophytes.

| Lithostratigraphy | Sections | Depth (m) | HG | HD | TLF | UF | XP | H' | Fs/X | Marine |
|---|---|---|---|---|---|---|---|---|---|---|
| Codó Formation | PR-1 | 1507,6 | 15,7 | 1,5 | 31,0 | 14,2 | 37,6 | 2,26 | 0,31 | 0 |
| | | 1509,7 | 19,6 | 0,5 | 8,2 | 29,4 | 42,3 | 2,19 | 0,32 | 0 |
| | | 1510,6 | 15,4 | 0,0 | 22,0 | 15,4 | 47,3 | 1,88 | 0,25 | 0 |
| | | 1513,1 | 6,6 | 2,0 | 20,2 | 13,1 | 58,1 | 2,04 | 0,13 | 0 |
| | PE-1 | 1562,0 | 44,4 | 0,0 | 8,7 | 33,2 | 13,8 | 2,59 | 0,76 | 0 |
| | | 1566,0 | 14,4 | 0,6 | 2,2 | 30,0 | 52,8 | 2,21 | 0,22 | 0 |
| | | 1568,5 | 4,2 | 0,0 | 20,8 | 16,7 | 58,3 | 1,99 | 0,07 | 0 |
| | | 1570,0 | 4,1 | 0,0 | 2,4 | 24,1 | 69,4 | 1,90 | 0,06 | 0 |
| | RL-1 | 1173,5 | 1,6 | 0,0 | 23,8 | 6,3 | 68,3 | 2,22 | 0,02 | 0 |
| | | 1174,1 | 12,0 | 4,0 | 10,0 | 12,0 | 62,0 | 2,06 | 0,21 | 0 |
| | | 1175,5 | 20,0 | 0,0 | 14,5 | 1,8 | 63,6 | 2,63 | 0,24 | 0 |
| | | 1235,25 | 18,8 | 1,6 | 10,2 | 7,8 | 61,7 | 2,57 | 0,25 | 1 |
| | | 1237,0 | 19,8 | 0,0 | 4,9 | 14,2 | 61,1 | 2,61 | 0,24 | 0 |
| | | 1239,5 | 27,0 | 1,6 | 6,3 | 6,3 | 58,7 | 1,85 | 0,33 | 0 |
| | | 1240,3 | 11,2 | 0,5 | 13,8 | 5,9 | 68,6 | 1,91 | 0,15 | 0 |
| | CI-1 | 820,6 | 6,5 | 0,0 | 15,7 | 0,0 | 77,8 | 1,78 | 0,08 | 0 |
| | | 834,5 | 3,7 | 0,0 | 3,7 | 0,0 | 92,6 | 1,30 | 0,04 | 0 |
| | | 836,0 | 0,0 | 0,0 | 0,0 | 10,2 | 89,8 | 1,66 | 0,00 | 0 |
| | | 837,0 | 14,7 | 2,7 | 6,0 | 48,9 | 27,7 | 2,28 | 0,18 | 0 |
| | | 838,0 | 15,8 | 0,0 | 1,5 | 9,8 | 72,9 | 1,74 | 0,06 | 0 |
| | | 845,0 | 4,8 | 0,0 | 1,4 | 23,3 | 70,5 | 2,07 | 0,33 | 0 |
| | | 855,0 | 5,2 | 0,0 | 5,2 | 5,2 | 84,5 | 1,10 | 0,13 | 0 |
| | | 855,9 | 10,8 | 0,6 | 10,1 | 3,8 | 74,7 | 2,11 | 0,38 | 0 |
| | | 857,6 | 21,6 | 2,6 | 4,2 | 31,6 | 40,0 | 2,64 | 0,10 | 1 |
| | | 866,55 | 8,6 | 0,5 | 5,6 | 6,6 | 78,8 | 2,27 | 0,25 | 1 |
| | | 866,65 | 16,9 | 1,6 | 4,4 | 21,3 | 55,7 | 2,26 | 0,21 | 0 |
| | | 867,8 | 16,0 | 0,0 | 16,6 | 7,1 | 60,4 | 2,83 | 0,39 | 0 |
| | | 888,75 | 19,3 | 0,0 | 12,9 | 22,9 | 45,0 | 2,28 | 0,30 | 0 |
| Bragança Formation | VN-1 | 1287,9 | 55,0 | 0,0 | 0,0 | 5,0 | 40,0 | 1,56 | 0,58 | 0 |
| | | 1289,88 | 18,4 | 0,0 | 5,3 | 18,4 | 57,9 | 1,94 | 0,24 | 0 |
| | | 1315,7 | 6,7 | 0,6 | 1,2 | 15,3 | 76,1 | 1,57 | 0,09 | 0 |
| | | 1317,69 | 33,3 | 0,0 | 0,0 | 0,0 | 66,7 | 1,29 | 0,33 | 0 |
| | EGST-1 | 676,44 | 19,2 | 0,5 | 14,8 | 54,4 | 11,0 | 2,54 | 0,64 | 0 |
| | | 732,3 | 30,1 | 2,4 | 3,0 | 8,4 | 56,0 | 2,65 | 0,37 | 0 |
| | | 733,3 | 8,1 | 0,0 | 4,3 | 7,6 | 80,0 | 1,48 | 0,09 | 0 |
| | | 735,3 | 13,7 | 3,0 | 0,5 | 12,2 | 70,6 | 1,97 | 0,19 | 0 |
| | | 1017,7 | 25,6 | 1,2 | 0,6 | 22,6 | 50,0 | 2,42 | 0,35 | 0 |
| | | 1789,1 | 19,0 | 0,0 | 1,7 | 6,3 | 73,0 | 1,83 | 0,21 | 0 |
| | | 1791,0 | 26,7 | 0,0 | 4,4 | 6,7 | 62,2 | 1,92 | 0,30 | 0 |
| | | 1846,0 | 57,1 | 0,0 | 14,3 | 14,3 | 14,3 | 1,95 | 0,80 | 0 |